Chemical Geology 525 (2019) 245–259

Contents lists available at ScienceDirect

Chemical Geology

journal homepage: www.elsevier.com/locate/chemgeo

Temporal evolution of primordial tungsten-182 and $^{3}He/^{4}He$ signatures in the Iceland mantle plume

A. Mundl-Petermeier[a,b,*], R.J. Walker[a], M.G. Jackson[c], J. Blichert-Toft[d], M.D. Kurz[e], S.A. Halldórsson[f]

[a] Department of Geology, University of Maryland, College Park, USA
[b] Department of Lithospheric Research, University of Vienna, Vienna, Austria
[c] Department of Earth Science, University of California Santa Barbara, USA
[d] Laboratoire de Géologie de Lyon, Ecole Normale Supérieure de Lyon and CNRS, France
[e] Woods Hole Oceanographic Institution, Woods Hole, USA
[f] NordVulk, Institute of Earth Sciences, University of Iceland, Iceland

ARTICLE INFO

Editor: Catherine Chauvel

Keywords:
$\mu^{182}W$
Iceland
Mantle plume
$^{3}He/^{4}He$
Primordial reservoir

ABSTRACT

Studies of short-lived radiogenic isotope systems and noble gas isotopic compositions of plume-derived rocks suggest the existence of primordial domains in Earth's present-day mantle. Tungsten-182 anomalies together with high $^{3}He/^{4}He$ in Phanerozoic rocks from large igneous provinces and ocean island basalts demonstrate the preservation of early-formed (within the first 60 Ma of solar system history) mantle domains tapped by modern mantle plumes. It has proven difficult to link the evidence for primordial domains with geochemical evidence for more recent processes, such as recycling. The Greenland-Iceland plume system, starting with eruptions of the Paleocene North Atlantic Igneous Province, is later manifested in the mid-Miocene to modern volcanic products of Iceland. Here, we report Pb isotopic compositions, $\mu^{182}W$ (deviations in $^{182}W/^{184}W$ of a sample from a laboratory reference standard in parts per million), and $^{3}He/^{4}He$, as well as highly siderophile element concentrations and Re-Os isotopic systematics of basaltic samples erupted at different times during the ~60 Ma history of the Greenland-Iceland plume. Paleocene samples from Greenland, representing the early stage of the mantle plume, are characterized by variable $^{3}He/^{4}He$ ranging from 7 to 48 R/R_A (measured $^{3}He/^{4}He$ normalized to the atmospheric ratio) and an average $\mu^{182}W$ of -4.0 ± 3.6 (2SD), within modern upper mantle-like values of 0 ± 4.5. The basalts from Iceland can be divided into two groups based on their Pb isotope compositions. One group, consisting mostly of Miocene basalts, is characterized by $^{206}Pb/^{204}Pb$ ranging from ~18.4 to 18.5, $^{3}He/^{4}He$ ranging from 17.8 to 40.2 R/R_A, and $\mu^{182}W$ values ranging from $+1.7$ to -9.1 ± 4.5. The other group, consisting mainly of Pleistocene and Holocene basalts, is characterized by higher $^{206}Pb/^{204}Pb$, ranging from ~18.7 to 19.2, $^{3}He/^{4}He$ ranging from 7.9 to 25.7 R/R_A, and $\mu^{182}W$ values ranging from -0.6 to -11.7 ± 4.5. Collectively, the Greenland-Iceland suite examined requires mixing between a minimum of three mantle source domains characterized by distinct Pb-He-W isotopic compositions, in order to account for this range of isotopic data. The temporal changes in the isotopic data for these rocks appear to track the dominant contributing plume components as the system evolved. One of the domains is indistinguishable from the ambient upper oceanic mantle and contributed substantial material throughout the time progression. The other two domains are most likely primordial reservoirs that underwent limited de-gassing. Given the negative $\mu^{182}W$ values in some rocks, one of these domains likely formed within the first 60 Ma of solar system history and is a major contributor to the youngest basalts. The isotopic characteristics of Greenland-Iceland plume-derived rocks reveal episodic changes in the source component proportions.

1. Introduction

Hafnium-182 decays to ^{182}W with a half-life of ~9 Ma (Vockenhuber et al., 2004). The parent isotope, therefore, was effectively extinct ~60 Ma into solar system (SS) history. Despite the short lifetime of ^{182}Hf, anomalies in ^{182}W have been observed in a variety of ancient terrestrial rocks (Willbold et al., 2011; Touboul et al., 2012; Touboul et al., 2014; Willbold et al., 2015; Rizo et al., 2016a;

* Corresponding author at: Department of Lithospheric Research, University of Vienna, Vienna, Austria.
E-mail address: andrea.mundl@univie.ac.at (A. Mundl-Petermeier).

https://doi.org/10.1016/j.chemgeo.2019.07.026
Received 25 April 2019; Received in revised form 13 July 2019; Accepted 22 July 2019
Available online 24 July 2019

Dale et al., 2017; Mundl et al., 2018; Tusch et al., 2019). These anomalies could have resulted from processes that fractionated Hf from W while ^{182}Hf was extant, including metal-silicate segregation and silicate-silicate fractionation. Alternatively, the ^{182}W isotopic composition of portions of the early mantle could have been initially established, or subsequently modified by the heterogeneous addition of late accreted materials (Willbold et al., 2011; Marchi et al., 2018). Both positive and negative ^{182}W anomalies in ancient rocks have been variably attributed to each of these general types of processes (e.g., Willbold et al., 2011; Touboul et al., 2012; Puchtel et al., 2016; Dale et al., 2017).

Anomalous ^{182}W isotopic compositions have also been detected in some Phanerozoic ocean island basalts (OIB), as well as continental and oceanic flood basalts (Rizo et al., 2016b; Mundl et al., 2017; Mei et al., 2018), indicating that portions of Earth's interior have retained Hf-W isotope characteristics established during the earliest stages of Earth history. Of note, the observed negative correlation of ^{182}W isotopic compositions with ^{3}He/^{4}He for OIB from Samoa and Hawaii links ^{182}W anomalies with a noble gas isotopic ratio that is consistent with derivation from a primordial mantle domain that has undergone considerably less degassing than the upper mantle (Mundl et al., 2017).

Iceland is an unusual OIB system that is commonly interpreted to have formed as a result of both hotspot and active ridge volcanism. Prior studies of mostly Pleistocene and Holocene basalts have reported elemental and isotopic heterogeneities within the mantle beneath Iceland representing depleted and enriched components (e.g., Hemond et al., 1993). Light rare earth element depleted rocks potentially indicate melting of recycled oceanic lithosphere that has previously experienced melt extraction (e.g., Skovgaard et al., 2001). In contrast, incompatible element enriched samples indicate involvement of a geochemically enriched mantle component (e.g., Debaille et al., 2009). Noble gas systematics of Icelandic basalts suggest contributions from a primordial mantle component characterized by comparatively unradiogenic He and Ne isotopes (e.g., Breddam et al., 2000; Moreira et al., 2001; Mukhopadhyay, 2012; Harðardóttir et al., 2018).

To further investigate the nature of the mantle sources feeding the Iceland volcanic system we report ^{182}W isotopic compositions of basalts that erupted during the Miocene, Pleistocene and Holocene at several different locations on the island. Additionally, we report ^{182}W data for samples from West and East Greenland that erupted during the Paleocene, ca. 60 Ma ago as part of the North Atlantic Igneous Province (NAIP; Fig. 1a–b). These rocks were likely generated by an early stage of volcanism from the same plume that subsequently formed Iceland (Marty et al., 1998; Graham et al., 1998; Starkey et al., 2009). We combine this data set with new and previously published ^{3}He/^{4}He and highly siderophile element (HSE) data, as well as Pb and Os isotopic compositions, in order to examine the contributions of several distinct mantle source materials to basalt production as the plume system evolved.

2. Samples

Sixteen Icelandic basalts and picrites were analyzed for W concentrations and ^{182}W isotopic compositions (Table 1). Of these, 11 were also analyzed for HSE concentrations and ^{187}Os isotopic compositions. Lead and He isotopic compositions were measured for most of the samples for which no such data had been previously published (Table 2). The basalts from Iceland represent two age groups (Fig. 1b): (i) eight samples from the northwestern part of Iceland, of which seven erupted during the mid-Miocene (406814, 406816, 406817, ICE-14-18, ICE-14-27, ICE-14-29, and ICE-16-03), and one sample (ICE-14-16) of a dike of unknown age that intruded into the Miocene basalts; and (ii) seven subglacially erupted Pleistocene samples from the Reykjanes Peninsula (RP; STAP-1), the Western Rift Zone (WRZ; ICE-14-32A), the Eastern Rift Zone (ERZ; A27), and the South Iceland Volcanic Zone (SIVZ; TRI-1, TRI-2 and THOR-1), as well as the off-rift Snæfellsnes Volcanic Zone (SNVZ; SNS214), and one Holocene basalt from the SNVZ (SNS206). Some major and trace element data, as well as radiogenic and stable isotope compositions of the neovolcanic Icelandic samples studied here, were previously reported by Debaille et al. (2009) and Halldórsson et al. (2016a, b). Notably, sample ICE-14-32A is from a well-studied unit, the Dagmálafell-Miðfell subglacial ridge in the WRZ (e.g., Burnard and Harrison, 2005; Mukhopadhyay, 2012). All studied samples are tholeiitic in composition with the exception of those from the SIVZ and the SNVZ, which are transitional-alkalic to alkalic, respectively (e.g., Halldórsson et al., 2016).

In addition to the samples from Iceland, we analyzed five samples from West and East Greenland (Table 1). These rocks are likely the volcanic products of an early stage of the Iceland mantle plume (e.g., Marty et al., 1998; Graham et al., 1998; Starkey et al., 2009; Fig. 1a). Further details regarding samples from West and East Greenland, such as major and trace element concentrations and isotopic compositions, can be found in Upton et al. (1980), Thirlwall et al. (1994), Ellam et al. (1998), Graham et al. (1998), Marty et al. (1998), Dale et al. (2009), Starkey et al. (2009), Larsen and Pedersen (2009), and Pedersen et al. (2017) (see supplementary material for details).

3. Analytical methods

3.1. Lead isotopic compositions

The Pb isotope compositions were determined on 200 mg of 0.5 to 1 mm-sized rock chips by wet chemistry and a *Nu Plasma 500 HR* multiple-collector inductively coupled plasma mass spectrometer using Tl doping and sample–standard bracketing (Albarède et al., 2004) at the Ecole Normale Supérieure in Lyon. Prior to attacking the samples in a 3:1:0.5 mixture of double-distilled concentrated HF, HNO_3, and $HClO_4$, they were leached for about an hour in hot 6 M HCl, including multiple ultrasonicating steps. After fuming with double-distilled concentrated $HClO_4$ to eliminate fluorides from the sample digestion procedure, the samples were taken up in 6 M HCl, placed on a hot plate at 130 °C until in complete solution, and evaporated to dryness. Lead was separated by ion-exchange chromatography on 0.5 ml columns filled with *Bio-Rad* AG1-X8 (100–200 mesh) resin using 1 M HBr to elute the sample matrix and 6 M HCl to collect the Pb. The total procedural Pb blank was < 20 pg. The NIST 981 Pb standard and the values of Eisele et al. (2003) were used for bracketing the unknowns (every two samples), while added Tl was used to monitor and correct for instrumental mass bias. The external reproducibility, estimated from the repeated NIST 981 measurements, was 100–200 ppm (or 0.01–0.02%) for ratios based on 204 (^{206}Pb/^{204}Pb, ^{207}Pb/^{204}Pb, ^{208}Pb/^{204}Pb), and 50 ppm (or 0.005%) for ^{207}Pb/^{206}Pb, ^{208}Pb/^{206}Pb, and ^{207}Pb/^{208}Pb.

3.2. Helium isotopic compositions

New He isotope data on olivine phenocrysts were obtained at the Woods Hole Oceanographic Institution following the method of Kurz et al. (2004). Between 240 and 350 mg olivine per sample were separated (Table S1) by hand-picking, cleaned in ethanol, and subsequently crushed in vacuo, releasing gases from melt and fluid inclusions. The He released by crushing was measured in a fully-automated dual collection magnetic sector mass spectrometer dedicated exclusively to He. The samples were bracketed by air standards (^{3}He/^{4}He = 1 Ra = 1.384×10^{-6}). Due to the relatively low helium concentrations, a secondary standard with ^{3}He/^{4}He = 8.35 Ra was also run periodically. The blanks were typically between 2-3 × 10^{-11} ccSTP/^{4}He, resulting in small blank corrections for these samples.

3.3. Tungsten concentrations and isotopic compositions

Tungsten concentrations were determined by isotope dilution at the University of Maryland. Approximately 100 mg of sample were digested

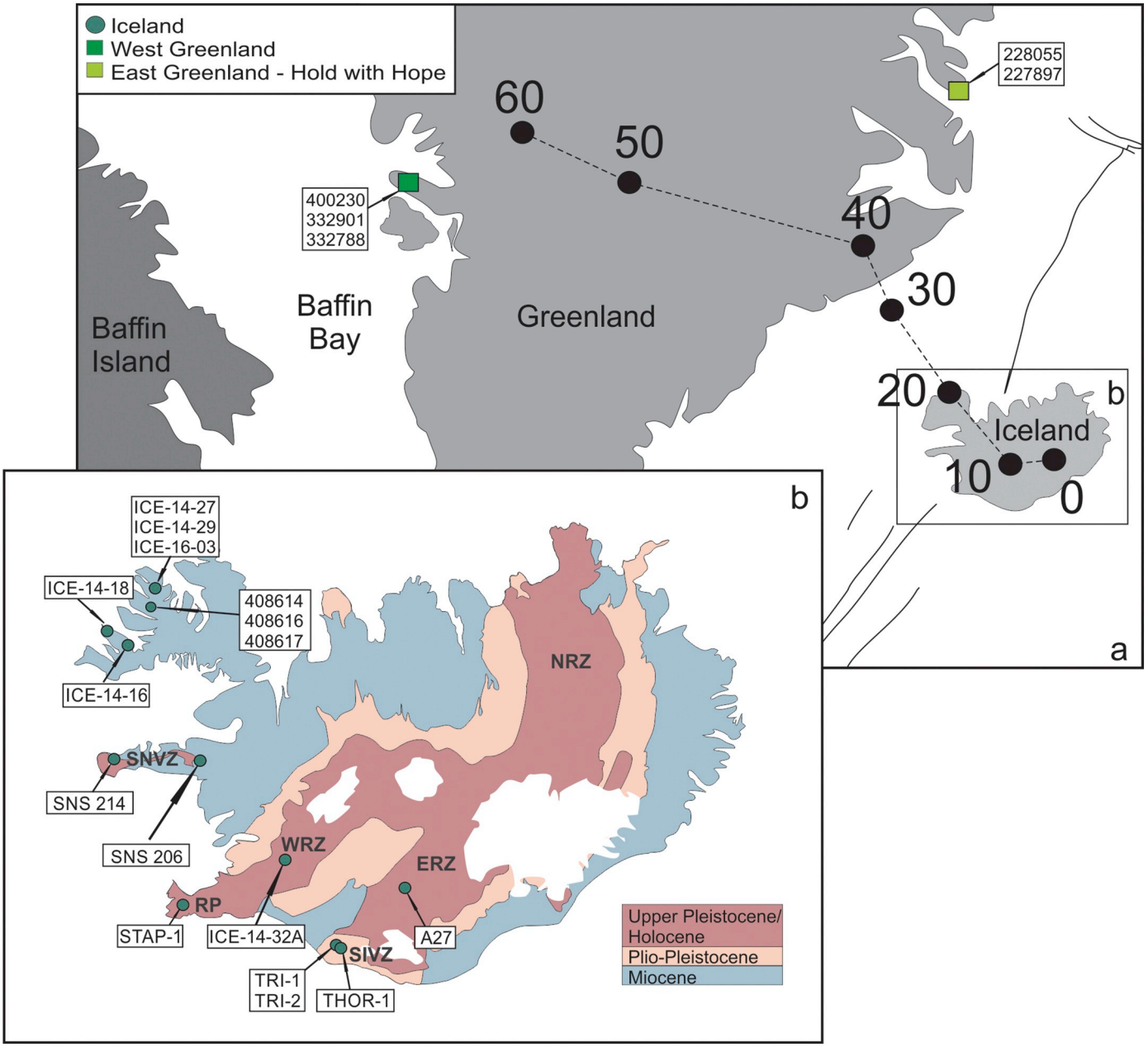

Fig. 1. (a) Sketch map of the North Atlantic Igneous Province (NAIP) showing the proposed track of the Iceland mantle plume. The black dots with numbers refer to the position of the mantle plume at that time in Ma from Saunders et al. (1997). Light green and dark green squares represent the East and West Greenland sample localities, respectively. (b) Map of Iceland showing the localities of the studied samples. The map is modified from Harðardóttir et al. (2018). All Iceland samples were erupted during the Miocene, Pleistocene, and Holocene. SNVZ – Snæfellsnes Volcanic Zone; RP – Reykjanes Peninsula; WRZ – Western Rift Zone; NRZ – Northern Rift Zone; ERZ – Eastern Rift Zone; SIVZ – South Iceland Volcanic Zone. (For interpretation of the references to color in this figure legend, the reader is referred to the web version of this article.)

together with a ^{182}W spike in ~6 ml of 5:1 concentrated HF:HNO_3 for 3 days at ~150 °C. After complete dissolution to a clear solution, samples were dried down and converted to chloride form by addition of ~2 ml of 6 M HCl and subsequently evaporated to dryness. Residues were then re-dissolved in 0.5 M HCl-0.5 M HF, and W was separated using an anion-exchange column chemistry procedure similar to that described in Kleine et al. (2004). Tungsten concentrations were measured using the *Element 2* single-collector ICP-MS at the University of Maryland. Resulting uncertainties on concentrations are typically < 5%.

For the determination of W isotopic compositions, between 3.5 and 55 g of sample powder was digested using 50–600 ml of a 5:1 mixture of concentrated HF and HNO_3 for 5 days at ~150 °C. After evaporation to dryness, samples were treated with concentrated HNO_3 and several drops of H_2O_2 to remove organics. The dried residues were then converted to chloride form by adding 1–30 ml of 8 M HCl. After subsequent evaporation to dryness, samples were re-dissolved in 40–360 ml of 1 M HCl-0.1 M HF and centrifuged. Tungsten was separated from the supernatant using a four-step ion exchange chromatography method described in Peters et al. (2019). Total W recovery was between 70 and 90% for all samples.

Isotopic compositions were measured by thermal ionization mass spectrometry in negative ionization mode (N-TIMS) using a *Thermo-Fisher Triton* at the University of Maryland. Samples were analyzed using the method described in Archer et al. (2017). All data are reported as $\mu^{182}W$, which is the deviation of $^{182}W/^{184}W$ of a given sample

Table 1
Helium and W isotopic compositions and concentrations of the studied samples from Iceland and Greenland. R/R_A is the measured $^3He/^4He$ normalized to the atmospheric composition. $\mu^{182}W$ and $\mu^{183}W$ are the deviations of a given sample's $^{182}W/^{184}W$ and $^{183}W/^{184}W$, respectively, from those of a terrestrial standard in ppm. $\mu^{182}W$ and $\mu^{183}W$ are normalized to $^{186}W/^{183}W$ and $^{186}W/^{184}W$, respectively. 2SE represents the internal run precision of individual analyses. 2SD is the 2× standard deviation of the Alfa Aesar standard solution analyzed during each analytical campaign. Previously published data from [1]Mundl et al. (2017), [2]Füri et al. (2010), [3]Williams (2005), [4]Halldórsson et al. (2016a), [5]Starkey et al. (2009), [6]Graham et al. (1998), [7]Marty et al. (1998) [8]Larsen and Pedersen (2009), [9]Ellam et al. (1998), [10]Thirlwall et al. (1994). Note that He isotopic ratios of subglacial basalts STAP-1, THOR-1 and TRI-2, reported by Halldórsson et al. (2016b) have been corrected for the presence of air-derived helium following methods described therein. All other helium isotope data, new and previously published, were obtained by *in-vacuo* crushing of olivine crystals.

Sample	$^3He/^4He$	1σ	^4He (ccSTP/g)	$\mu^{182}W_{6/3}$	2SE	2SD of Stds (N)	$\mu^{183}W_{6/4}$	2SE	2SD of Stds (N)	W conc [ppb]	MgO [wt%]
Iceland											
408614[1]	40.2	0.7	4.993E-09	−7.1	4.0		1.9	4.1		59.3	12.1
408616	38.7	1.0	7.44E-10	−9.3	2.9	2.7 (4)	−4.7	3.4	6.6 (4)	34	14.5
408617				−6.7	3.4	3.0 (3)	0.5	3.8	3.4 (3)		
408617_2				−7.8	6.5	5.7 (4)	3.1	8.7	3.3 (4)		
408617 ave	37.6	0.8	1.844E-09	−7.2			1.8			48	16.6
A27	19.7[2]		1.887E-07	−4.8	4.2	4.3 (9)	4.1	4.4	5.6 (9)	117	6.3[4]
ICE-14-16				−10.1	3.8	3.0 (3)	0.1	4.9	3.4 (3)	76	
ICE-14-16_2				−13.4	4.2	5.7 (4)	−2.3	5.0	3.3 (4)	72	
ICE-14-16 ave	19.8	0.4	3.179E-09	−11.7			−1.1			74	5.0
ICE-14-18				−4.4	3.2	3.0 (3)	−0.1	3.4	3.4 (3)		
ICE-14-18_2				−4.6	3.3	5.7 (4)	2.5	4.0	3.3 (4)		
ICE-14-18 ave	26.3	0.7	7.271E-10	−4.5			1.2			62	8.1
ICE-14-27	36.6	1.0	5.868E-10	−6.5	3.3	2.7 (4)	2.1	4.1	6.6 (4)	49	9.2
ICE-14-29	34.2	1.0	5.001E-10	−8.7	2.8	2.7 (4)	4.2	3.4	6.6 (4)	46	10.6
ICE-14-32A[1]	17.8	0.3	7.58E-09	1.7	4.4		1.0	5.1		9	
ICE-14-32A dup										8	n.d.
ICE-16-03				−8.8	4.0	3.0 (3)	−4.8	4.6	3.4 (3)		
ICE-16-03_2				−6.9	3.3	5.7 (4)	6.9	3.7	3.3 (4)		
ICE-16-03 ave	36.1	1.0	1.308E-09	−7.8			1.0			33	18.8
SNS206	8.5[3]	0.1	8.46E-09	−0.6	3.2	5.5 (7)	3.3	3.6	4.8 (7)	380	9.1[3]
SNS214	7.9[3]	0.2	3.00E-09	−0.7	3.5	5.5 (7)	0.9	4.0	4.8 (7)	398	9.9[3]
STAP-1	14.2[4]		4.84E-08	−3.5	3.4	5.5 (7)	5.7	3.9	4.8 (7)	285	7.8[4]
THOR-1	3.7[4]		3.40E-10	−12.9	3.6	3.8 (6)	−1.6	4.5	7.7 (6)	339	4.3
TRI-1				−10.9	3.2	3.8 (6)	−3.6	3.6	7.7 (6)		
TRI-1_2				−11.6	5.0	2.8 (3)	−3.2	5.4	2.6 (3)		
TRI-1 ave	25.3[4]	0.6	4.73E-07	−11.2			−3.4			290	5.5
TRI-2				−9.4	2.9	3.8 (6)	1.4	3.3	7.7 (6)		
TRI-2_2				−9.7	4.1	2.6 (4)	2.4	4.6	3.9 (4)		
TRI-2 ave	25.7[4]	0.6	1.23E-07	−9.5			1.9			199	7.5[4]
Greenland											
400230				−1.8	3.1	4.3 (6)	0.6	3.7	6.8 (6)		
400230_2				−1.7	3.5	2.9 (4)	1.2	4.5	3.6 (4)		
400230 ave	48[5]	1.3	1.27E-08	−1.8			0.9			21.9	20.6[5]
332901				−7.8	3.1	4.3 (6)	−0.2	3.9	6.8 (6)		
332901_dup				−4.6	3.3	2.9 (4)	−0.9	4.5	3.6 (4)		
332901 ave	46[5]	1.0	1.75E-08	−6.2			−0.6			37.5	24.6[5]
332788				−6.5	3.6	2.9 (4)	−4.5	4.7	3.6 (4)		
332788_2				−3.2	3.2	3.9 (4)	1.0	3.6	8.0 (4)		
332788 ave	30.4[6]	0.5	3.87E-08	−4.8			−1.8			36.3	25.6[8]
228055				−3.2	3.5	2.9 (4)	−3.8	4.2	3.6 (4)		
228055_2				−6.2	3.4	3.9 (4)	−4.2	4.2	8.0 (4)		
228055 ave	20[7]	0.7	1.97E-08	−4.7			−4.0			103.3	20.1[9]
227987				−1.8	3.5	2.9 (4)	1.2	4.3	3.6 (4)		
227987_2				−3.3	3.5	3.9 (4)	−0.4	3.6	8.0 (4)		
227987 ave	7[7]	1.0	2.80E-09	−2.6			0.4			126.3	17.0[10]

from that of the in-house *Alfa Aesar* laboratory W standard in parts per million. In addition to repeated analyses of laboratory standard solutions to determine the external reproducibility, steel standard NIST129c was processed and analyzed to monitor potential fractionation processes taking place during chromatographic column chemistry. The determined $^{182}W/^{184}W$ and $^{183}W/^{184}W$ ratios are identical within uncertainties to the average *Alfa Aesar* standard data (Table S2). This result, combined with the lack of ^{183}W anomalies in any samples processed for this study, leads to the conclusion that the isotopic compositions were not modified by nuclear field shift effects, as proposed for a similar method by Kruijer and Kleine (2018).

3.4. Highly siderophile element concentrations and Os isotopic compositions

For the determination of Re-Os isotopic compositions and HSE abundances, ~1 g of whole-rock powder per sample was digested in a mixture of 5 ml of concentrated HNO_3 and 4 ml of concentrated HCl, together with appropriate amounts of ^{185}Re, ^{190}Os, and HSE (^{99}Ru, ^{105}Pd, ^{191}Ir, ^{194}Pt) spikes in sealed 25 ml Pyrex™ borosilicate Carius tubes, heated to 250 °C for 3 days. Osmium was separated from the acid solution by CCl_4 solvent extraction (Cohen and Waters, 1996), back-extracted into concentrated HBr, and purified by microdistillation from a chromic acid solution (Birck et al., 1997). Rhenium, Ir, Ru, Pt, and Pd were separated and purified using an anion-exchange chromatography protocol similar to that of Rehkämper and Halliday (1997).

Osmium isotopic analyses were carried out by negative thermal ionization mass spectrometry using a secondary electron multiplier detector of a *Thermo Fisher Triton* mass spectrometer at the University of Maryland. The long-term external precision on equivalent quantities of an Os laboratory standard was 0.1% (2SD, $n = 64$). The in-run precision

Table 2
Highly siderophile element concentrations [ppb], Re-Os and Pb isotopic compositions and bulk rock (glass for subglacial glasses) MgO [wt%] of Iceland samples. #ages for the calculation of initial $^{187}Os/^{188}Os$ taken from published values of samples in close vicinity. *b.d.l. – below detection limit. Previously published data from: MgO, Os and Re concentrations and Re-Os isotopic data for samples SNS206 and SNS214 (average of 2 analyses) from [1]Debaille et al. (2009). [2]Halldórsson et al. (2016a); [3] $^{206}Pb/^{204}Pb$ taken from sample MID-1 Halldórsson et al. (2016a), which was collected from the same sample outcrop as ICE-14-32A. [4]A range of Pb isotope ratios approximated from nearby flows of similar age; [5]Graham (2002); [6]Marty et al. (1998).

Sample	Pb-Group	Os	Ir	Ru	Pt	Pd	Re	$^{187}Re/^{188}Os$	$^{187}Os/^{188}Os_{(m)}$	$^{187}Os/^{188}Os_{(i)}$ #	$^{206}Pb/^{204}Pb$	2σ	$^{207}Pb/^{204}Pb$	2σ	$^{208}Pb/^{204}Pb$	2σ	MgO
Iceland																	
408614	"*low-Pb64*"	2.811	0.450	0.761	4.219	3.088	0.279	0.478	0.13515	0.13503	18.5324	0.0023	15.4781	0.0018	38.2123	0.0046	12.1
408616	"*low-Pb64*"	n.d.	n.d.	n.d.	n.d.	n.d.	n.d.				18.5090	0.0022	15.4749	0.0041	38.1787	0.0109	14.5
408617	"*low-Pb64*"	2.019	0.290	0.727	3.330	4.614	0.316	0.755	0.13526	0.13506	18.5119	0.0024	15.4733	0.0025	38.2201	0.0060	16.6
A27	"*low-Pb64*"	n.d.	n.d.	n.d.	n.d.	n.d.	n.d.				18.4920[2]	0.0018	15.4730[2]	0.0028	38.1850[2]	0.0052	6.34
ICE-14-16	"*high-Pb64*"	0.190	0.112	0.060	5.533	2.904	0.432	10.98	0.14382	0.14162	18.7358	0.0007	15.5093	0.0007	38.4688	0.0022	5.0
ICE-14-18	"*low-Pb64*"	0.857	0.137	0.226	1.812	2.059	0.814	4.584	0.14307	0.14185	18.4903	0.0009	15.4785	0.0008	38.1800	0.0020	8.1
ICE-14-27	"*low-Pb64*"	0.831	0.221	0.184	4.057	4.380	0.260	1.511	0.13519	0.13479	18.4218	0.0014	15.4596	0.0020	38.1304	0.0019	9.2
ICE-14-29	"*low-Pb64*"	1.619	0.323	0.368	3.372	3.664	0.120	0.359	0.13320	0.13310	18.4483	0.0010	15.4631	0.0008	38.1498	0.0021	10.6
ICE-14-32A	"*low-Pb64*"	1.945	0.254	0.838	5.928	8.329	0.385	0.956	0.13347	0.13347	18.4873[3]		n.d.		n.d.		n.d.
ICE-16-03	"*low-Pb64*"	4.291	0.467	1.067	2.757	2.357	0.082	0.092	0.13304	0.13302	18.4724	0.0031	15.4664	0.0030	38.1784	0.0030	18.8
SNS206	"*high-Pb64*"	0.259[1]	n.d.	n.d.	n.d.	n.d.	0.258[1]			0.12891	18.95–19.05[4]		15.50–15.53[4]		38.50–38.65[4]		9.1
SNS214	"*high-Pb64*"	0.230[1]	n.d.	n.d.	n.d.	n.d.	0.211[1]			0.12629	18.92–18.98[4]		15.50–15.51[4]		38.50–38.60[4]		9.9
STAP-1	"*high-Pb64*"	n.d.	n.d.	n.d.	n.d.	n.d.	n.d.				18.881[2]		15.525[2]		38.483[2]		7.8
THOR-1	ungrouped	0.003	0.002	b.d.l.*	0.035	1.236	0.759	1438	0.33840	0.33600	n.d.		n.d.		n.d.		4.3
TRI-1	"*high-Pb64*"	0.049	0.025	0.010	0.301	0.140	1.157	114.5	0.16366	0.16290	n.d.		n.d.		n.d.		5.5
TRI-2	"*high-Pb64*"	0.489	0.253	0.201	2.698	6.169	0.982	9.693	0.13667	0.13660	19.1542	0.0020	15.5372	0.0020	38.7092	0.0060	7.5
Greenland																	
332788											18.105[5]		15.482[5]		38.043[5]		25.7
228055											18.22[6]		15.41[6]		37.83[6]		20.1
227987											18.51[6]		15.52[6]		38.40[6]		17.0

of the measured $^{187}Os/^{188}Os$ for all samples was between 0.1 and 0.3%. Rhenium, Ir, Ru, Pt, and Pd were analyzed on a single-collector ICP-MS (*Element 2*) at the University of Maryland. Total analytical blanks for Os, Re, Ir, Ru, Pt, and Pd were 0.6 pg, 1.0 pg, 0.9 pg, 11 pg, 8 pg, and 13 pg, respectively, which result in a blank contribution on the sample measurements of 0.01–0.6% (Os; except sample THOR-1 with 12%), 0.04–0.6% (Re), 0.09–1.7% (Ir; except sample THOR-1 with 20%), 0.5–9.3% (Ru; except sample TRI-1 with 54%), 0.07–1.4% (Pt; except sample THOR-1 with 12%) and 0.08–0.5% (Pd, except sample TRI-1 with 4.6%).

4. Results

4.1. Lead isotope systematics

The Pb isotopic compositions of the Icelandic basalts in this study can be divided into two groups with well-resolved isotopic compositions: a "*low-Pb64*" group and a "*high-Pb64*" group (Table 2). The Miocene samples from northwest Iceland, as well as upper Pleistocene samples ICE-14-32A and A27, are characterized by comparatively low $^{206}Pb/^{204}Pb$ ranging from ~18.4 to 18.5, defining the "*low-Pb64*" group. All other Pleistocene and Holocene basalts, as well as dike sample ICE-14-16 from northwest Iceland (unknown age), have higher $^{206}Pb/^{204}Pb$ ranging from ~18.7 to 19.2, defining the "*high-Pb64*" group. Lead isotopic data were not determined for THOR-1 and TRI-1. However, samples TRI-1 and TRI-2 are from the same subglacial formation and thus, the Pb isotopic composition determined for TRI-2 (Table 1 and Halldórsson et al., 2016a) is assumed to be representative of sample TRI-1. Hence, sample TRI-1 is included in the "*high-Pb64*" group. $^{207}Pb/^{204}Pb$ and $^{208}Pb/^{204}Pb$ can be similarly divided into the same two groups with ratios ranging from 15.46 to 15.48 and 38.13 to 38.22, respectively, for the "*low-Pb64*" group, and 15.51 to 15.53 and 38.47 to 38.67, respectively, for the "*high-Pb64*" group.

Previously published Pb isotopic data for three of the Paleocene samples from Greenland studied here are characterized by comparatively low $^{206}Pb/^{204}Pb$ with ratios ranging from 18.1 to 18.5 (Graham et al., 1998; Marty et al., 1998). Two of these lavas have lower $^{206}Pb/^{204}Pb$ than any members of the "*low-Pb64*" group from Iceland, but a third Greenland lava from East Greenland has a $^{206}Pb/^{204}Pb$ that falls within the range of the "*low-Pb64*" Iceland group. We consider the five Greenland lavas as a third group—in addition to the Iceland "*low-Pb64*" and "*high-Pb64*" groups, in the discussion below.

4.2. $^{3}He/^{4}He$ systematics

The entire sample suite is characterized by $^{3}He/^{4}He$ ranging from 3.7 to 48.0 R/R_A (where R/R_A is the measured $^{3}He/^{4}He$ normalized to the atmospheric ratio of 1.384×10^{-6}; Mabry et al., 2013; Table 1). Most samples have $^{3}He/^{4}He$ significantly higher than the average for mid-ocean ridge basalts (MORB; 7–9 R/R_A; Graham, 2002). $^{3}He/^{4}He$ ranges to higher values in the "*low-Pb64*" group (up to 40 R/R_A) than in the "*high-Pb64*" group (up to 25.7 R/R_A). These results are consistent with prior He isotope studies of the Iceland plume (e.g., Harðardóttir et al., 2018; Starkey et al., 2009).

Although we note that three of the six subglacial glasses have higher He concentrations relative to olivine crystals, no clear correlations are evident between ^{4}He concentrations and $^{3}He/^{4}He$ (Fig. S1), age or composition of the rock (e.g., MgO). We also note that one subglacial sample, THOR-1, with a low $^{3}He/^{4}He$ of 3.7 R_C/R_A (even after applying a correction for the presence of air-derived He; Halldórsson et al., 2016a; Table 1) falls well below $^{3}He/^{4}He$ ratios which are thought to be representative for unmodified samples from the SIVZ (generally > 20 R_A: see Harðardóttir et al., 2018). For an Icelandic subglacial glass, sample THOR-1 has a particularly low He concentration of 0.37×10^{-9} cm^3STP/g, and a low X-value ($[^{4}He/^{20}Ne_{sample}]/[^{4}He/^{20}Ne_{air}]$) of only 2.9, which likely resulted from extensive degassing prior to or during eruption (e.g., Harðardóttir et al., 2018). The low $^{3}He/^{4}He$ of this subglacial glass, likely reflects extensive atmospheric He contamination and possibly radiogenic ^{4}He in-growth. Thus, the He isotopic composition of THOR-1 is unlikely to be representative of its source composition.

East Greenland sample (227987) has MORB-like $^{3}He/^{4}He$ of 7 R/R_A (Marty et al., 1998). Despite the comparatively old age of this sample (~60 Ma), Marty et al. (1998) argued against post-eruptive modification of $^{3}He/^{4}He$ by degassing and subsequent radiogenic ^{4}He in-growth. Instead they suggested that the measured $^{3}He/^{4}He$ of 7 R/R_A likely results from the addition of radiogenic ^{4}He to the mantle plume and thus, reflects that at the time of eruption. In this case, we point out that MORB-like $^{3}He/^{4}He$ are also found in the neovolcanic zones of Iceland and likely represent mixing between plume- and upper mantle-derived He (e.g., Harðardóttir et al., 2018 and references therein).

Although the effects of secondary processes such as degassing, radiogenic in-growth, crustal contamination and/or addition of cosmogenic ^{3}He cannot be completely ruled out, particularly in the case of the Greenland and Mid-Miocene Iceland samples, for which the measured $^{3}He/^{4}He$ most likely represent the Icelandic mantle source compositions (see Harðardóttir et al., 2018). All of the new He measurements were obtained by in vacuo crushing of olivine phenocrysts, which is an effective method of minimizing cosmogenic and radiogenic contributions (see discussion in Supplementary material).

4.3. Tungsten concentrations and ^{182}W isotopic compositions

Tungsten concentrations for all samples analyzed range from 8 to 400 ppb (Table 1). Overall, the "*low-Pb64*" group Iceland samples and the Paleocene Greenland samples are characterized by generally low W concentrations ranging from 8 to 130 ppb. By comparison, the "*high-Pb64*" samples are characterized by higher W concentrations ranging from 200 to 400 ppb. The difference in concentration between the two Pb groups is likely not a reflection of differing degrees of partial melting or other crystal-liquid fractionation effects, given that both sample suites exhibit large variations in major element compositions, such as MgO and SiO_2, yet, there is no overlap in W concentrations. Further, even samples from the "*low-Pb64*" group, with MgO and SiO_2 contents similar to those from the "*high-Pb64*" group, show distinctly lower overall W concentrations (Table 2, Fig. S2).

For the entire Greenland and Iceland sample suite, $\mu^{182}W$ ranges from +1.7 to −12.9 ± 4.5 (where the uncertainty is the 2SD long-term external precision of standard measurements). Six samples are characterized by negative $\mu^{182}W$ values that are resolved from the 2SD of the laboratory standard value (defined as 0 ± 4.5 ppm), and 11 samples are resolved from the 2SE of the laboratory standard (defined as 0 ± 1 ppm) (Fig. 2, Table 1). By contrast, six Icelandic samples have $\mu^{182}W$ values that overlap with the 2SE of repeated analysis of the laboratory standard, which is assumed to be representative of the modern upper mantle. Both the "*low-Pb64*" and "*high-Pb64*" groups include samples with "normal" $\mu^{182}W$ values and resolved negative $\mu^{182}W$ values. The lowest $\mu^{182}W$ values for each of the Greenland, "*low-Pb64*" and "*high-Pb64*" groups broadly correlate with age. Most of the Paleocene basalts from East and West Greenland show no resolvable ^{182}W anomalies for both comparatively low and very high $^{3}He/^{4}He$ (up to 48 R/R_A), although two separate measurements of sample 332901 give an average $\mu^{182}W$ of −6.2 ± 4.6, which is resolved from the 2SE of repeated measurements of the laboratory standard (Fig. 3). Overall, these samples are characterized by an average value of −4.0 ± 3.6 (2SD). The"*low-Pb64*" Miocene Iceland samples have $\mu^{182}W$ values that range to as low as −9.3 ± 4.5, while the "*high-Pb64*" samples erupted during the Pleistocene and Holocene range to the lowest $\mu^{182}W$ value of −11.2 ± 4.5. Overall, the "*high-Pb64*" rocks display a larger range in $\mu^{182}W$ compared to the"*low-Pb64*" samples (Fig. S3).

The $\mu^{182}W$ values do not correlate with bulk rock major element compositions, such as MgO or SiO_2 (Fig. S4). Plots of $^{3}He/^{4}He$ versus

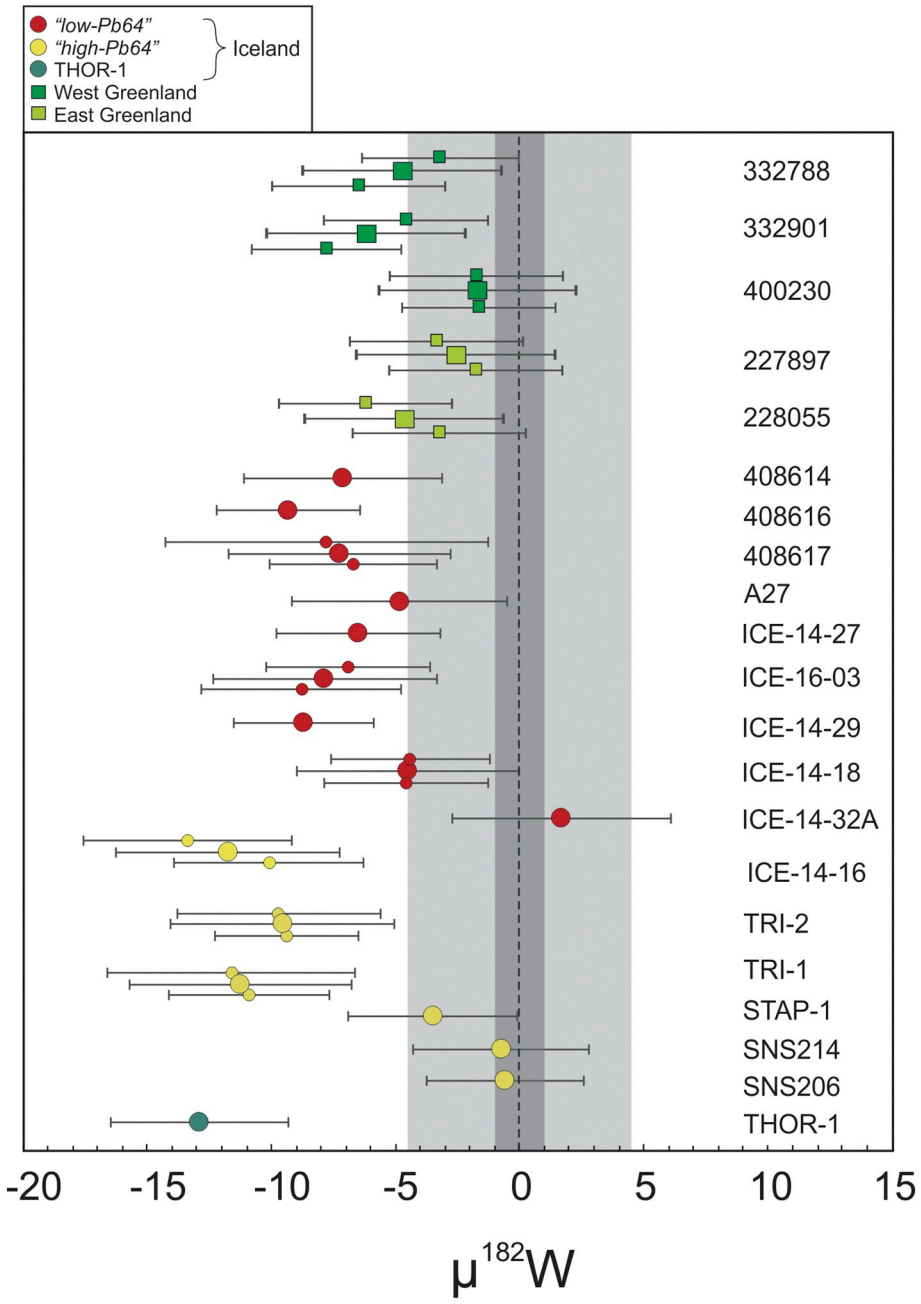

Fig. 2. $\mu^{182}W$ values for basalts from Iceland and Greenland. Error bars represent 2SE of individual sample runs or long-term external precision (2SD) for average analyses of multiple samples (± 4.5 ppm), whichever is larger. Small symbols represent separate loads of the same sample digestion or chemistry duplicates, with large symbols reflecting their averages. The light grey bar is the long-term external precision (2SD) of 4.5 ppm of the laboratory standard, while the dark grey bar is the 2SE (1 ppm) of the same laboratory standard. Light green and dark green squares represent the East and West Greenland samples, respectively. Yellow filled circles represent "*high-Pb64*" samples; red filled circles are samples from the "*low-Pb64*" group. As Pb isotopic data are unavailable for THOR-1, this samples was excluded from the groupings based on Pb isotope compositions. (For interpretation of the references to color in this figure legend, the reader is referred to the web version of this article.)

$\mu^{182}W$, on the other hand, suggest distinct negative trends for each of the "*low-Pb64*" and "*high-Pb64*" Iceland basalt groups (Figs. 3 & S5). All nine samples from the "*low-Pb64*" group form a shallow, negatively sloping trend, where the sample with the highest $^{3}He/^{4}He$ of 40 R/R_A has a $\mu^{182}W$ of −7.1 ± 4.5 (Table 1, Fig. 3). All six "*high-Pb64*" Icelandic samples define negative trend with a steeper slope compared to the "*low-Pb64*" samples that is indistinguishable from trends defined by basalts from Hawaii and Samoa (Fig. 3; Mundl et al., 2017).

The He-W data for the Greenland samples are characterized by large variations in $^{3}He/^{4}He$, yet an only slightly negative averaged $\mu^{182}W$ value. Collectively, these samples may define a third, horizontal trend on the He-W plot (Fig. 3).

4.4. Highly siderophile element concentrations and Os isotopic compositions

The "*low-Pb64*" group is characterized by distinctly higher Ir group-Pt group element (IPGE; Os, Ir, Ru) concentrations than the "*high-Pb64*" group with, for example, Os concentrations ranging from 0.8 to 4.3 ppb. In comparison, all "*high-Pb64*" group samples are characterized by Os abundances of < 0.5 ppb (Fig. S6). Bulk silicate Earth (BSE)-normalized HSE plots show up to several orders of magnitude lower IPGE concentrations in the "*high-Pb64*" samples, and also significantly lower Pt group-PGE (P-PGE; Pt, Pd) abundances in some samples, compared to the "*low-Pb64*" samples (Fig. 4). As with W concentrations, the differences remain even when comparing data for the two groups with similar MgO. For example, "*low-Pb64*" samples ICE-14-18, ICE-14-27 and ICE-14-29 have comparable MgO contents to "*high-Pb64*" samples TRI-2, SNS206 and SNS214. Yet, the former show considerably higher Os concentrations (Table 2). Thus, as with W concentrations, the differences in HSE concentrations are more likely a characteristic of the mantle source, than a result of melting or crystal-liquid fractionation processes.

Initial Os isotopic compositions are generally within the range reported by prior studies of Baffin Bay/West Greenland and Icelandic

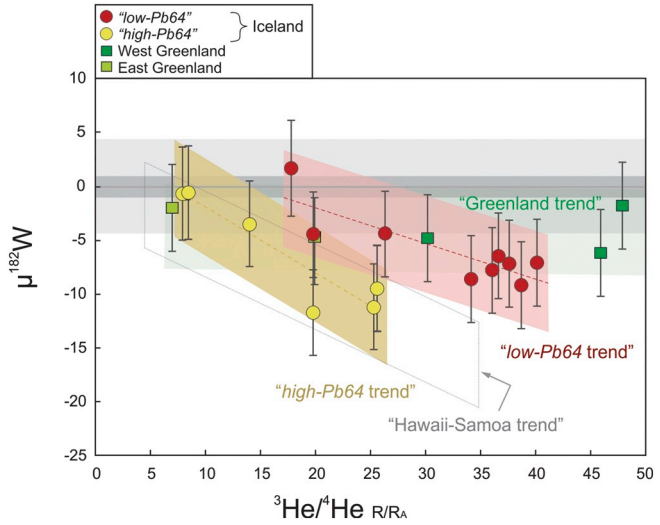

Fig. 3. $\mu^{182}W$ versus $^{3}He/^{4}He$ (R/R_A). Symbols as in Fig. 2. Where applicable, data points represent the average of two sample analyses. Error bars represent long-term external precision (2SD) for average analyses of multiple standards (± 4.5 ppm). Error bars for $^{3}He/^{4}He$ are smaller than the symbols. Samples from Iceland form two distinct W-He trends – a "*low-Pb64*" and a "*high-Pb64*" trend – that are discussed in the main text. Colored fields represent the error envelope of the different groups using the 2SD of standards (4.5 ppm). The light and dark grey fields represent the long-term external precision 2SD of 4.5 ppm and 2SE of 1 ppm, respectively, of the laboratory standard. For comparison, the black dashed line represents the trend for samples from Samoa and Hawaii from Mundl et al. (2017). Parameters for the "*low-Pb64*" and "*high-Pb64*" trends, respectively, are: $R^2 = 0.684$; slope = −0.322; y-intercept: 4.309 and $R^2 = 0.856$; slope = −0.605; y-intercept = 4.011.

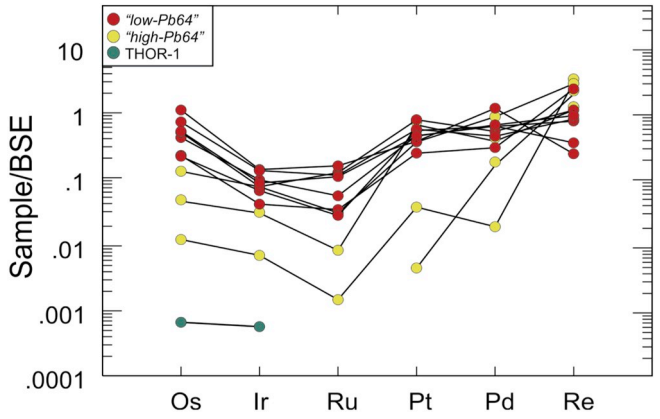

Fig. 4. Highly siderophile element abundances normalized to bulk silicate Earth (BSE) values from Becker et al. (2006). Most "*high-Pb64*" group samples show significantly lower Ir group-Pt group element (IPGE) abundances compared to the "*low- Pb64*" group samples. Symbols as in Fig. 2.

basalts (e.g., Brandon et al., 2007; Debaille et al., 2009; Dale et al., 2009; Fig. S7). While all samples analyzed in this study are characterized by supra-chondritic initial $^{187}Os/^{188}Os$, THOR-1, which, based on its location, likely belongs to the "*high-Pb64*" group, has a significantly higher calculated initial $^{187}Os/^{188}Os$ of 0.336. However, because of the very low Os concentration (3 ppt) of this sample, the Os isotopic composition may have been disturbed by secondary processes and thus, may not reflect its initial composition. With the exception of THOR-1, initial $^{187}Os/^{188}Os$ of both groups range from 0.133 to 0.162 and show no discernable differences between the "*low-Pb64*" and "*high-Pb64*" groups (Table 2, Figs. S6–7). The Os isotopic data also show no correlation with $^{3}He/^{4}He$ within the two groups, in contrast to the correlation noted for Icelandic picrites by Brandon et al. (2007).

5. Discussion

5.1. Origin of the Pb-He-W isotopic signatures in Icelandic samples

The NAIP is a result of complex igneous processes involving variable degrees of melting of multiple mantle sources, followed by subsequent crystal-liquid fractionation and in some cases crustal contamination. Based on the combination of long-lived radiogenic, noble gas and stable isotope systematics, as well as major and trace element compositions, various prior studies have advocated for contributions to this magmatic system from multiple sources that include deep mantle primordial domains, the depleted MORB mantle (DMM), recycled crust, and recycled enriched subcontinental lithospheric mantle (e.g., Graham et al., 1998; Brandon et al., 2007; Starkey et al., 2009; Debaille et al., 2009; Agranier et al., 2019).

The focus of this study is on the He-W isotopic systems that provide evidence for the involvement of primordial mantle domains. Collectively, the He-W isotopic characteristics of these samples require their derivation from a combination of mantle source domains with at least three disparate He-W isotopic characteristics (Fig. 3). With regards to He and W, one of the source domains is isotopically indistinguishable from the upper mantle (Fig. 5). Based on high $^{3}He/^{4}He$ in two of the remaining domains, and low $\mu^{182}W$ in one of these, it can be concluded that two primordial mantle domains also likely contributed to the Greenland-Iceland plume. The characteristics of these domains can be broadly established based on the most extreme isotopic and chemical compositions of the Greenland-Iceland suite.

The dichotomy in the Pb isotopic systematics, where "*low-Pb64*" group samples show small negative $\mu^{182}W$ signatures in combination with very high $^{3}He/^{4}He$, and samples from the "*high-Pb64*" group show lower $\mu^{182}W$ signatures at a given $^{3}He/^{4}He$, appears to be related to He-W isotopic systematics. This connection of Pb and He-W signatures reflected in individual sample groups makes it important to consider how the imprint of a long-lived radiogenic isotope system can be reconciled to the interpretation of the He-W systematics. Hence, it is important to review prior observations and interpretations regarding the causes of the Pb isotopic variations among Icelandic basalts. Several prior studies have proposed multiple mantle plume source components for Icelandic volcanic rocks (e.g., Schilling et al., 1982; Hanan and Schilling, 1997; Kerr et al., 1995; Chauvel and Hémond, 2000; Hanan et al., 2000). Observed variations in long-lived radiogenic isotope and trace element compositions have been ascribed to the heterogeneous nature of the Iceland mantle plume. Volcanic products have been interpreted to reflect mixtures of both geochemically depleted and enriched (lower) mantle source materials. Enriched mantle plume components have been interpreted to represent entrained subcontinental lithospheric mantle (Hanan et al., 2000) or ancient recycled oceanic crust (Chauvel and Hémond, 2000). A depleted plume source has been suggested to be intrinsic to the Iceland mantle plume and thus, is different from the North Atlantic MORB source (Kerr et al., 1995).

Based on Pb isotopes, Welke et al. (1968) first recognized that basalts from Iceland can be divided into two groups that correlate with age. Further studies of Icelandic basalts suggested episodic changes in Pb isotopic compositions (e.g., Schilling et al., 1982; Hanan and Schilling, 1997; Chauvel and Hémond, 2000). Hanan and Schilling (1997) identified two parallel trends of $^{206}Pb/^{204}Pb$ that reflect increasing $^{206}Pb/^{204}Pb$ from ~18.2 to 19.1 from 15 to 8 Ma ago in West and East Tertiary basalts, and a subsequent decrease in $^{206}Pb/^{204}Pb$ from 8 Ma to the end of the Tertiary in the East Tertiary basalts. They argued for episodic changes in the proportions of at least three different plume source components (depleted asthenosphere, radiogenic plume-derived and EM I-like components) leading to the changes in Pb isotope compositions. Cyclic variations of Pb isotope compositions continued through the Pleistocene and Holocene, and are to some extent spatially controlled within the neovolcanic zone at present (e.g., Kokfelt et al., 2006). For example, neovolcanic eruptions from SNVZ (samples

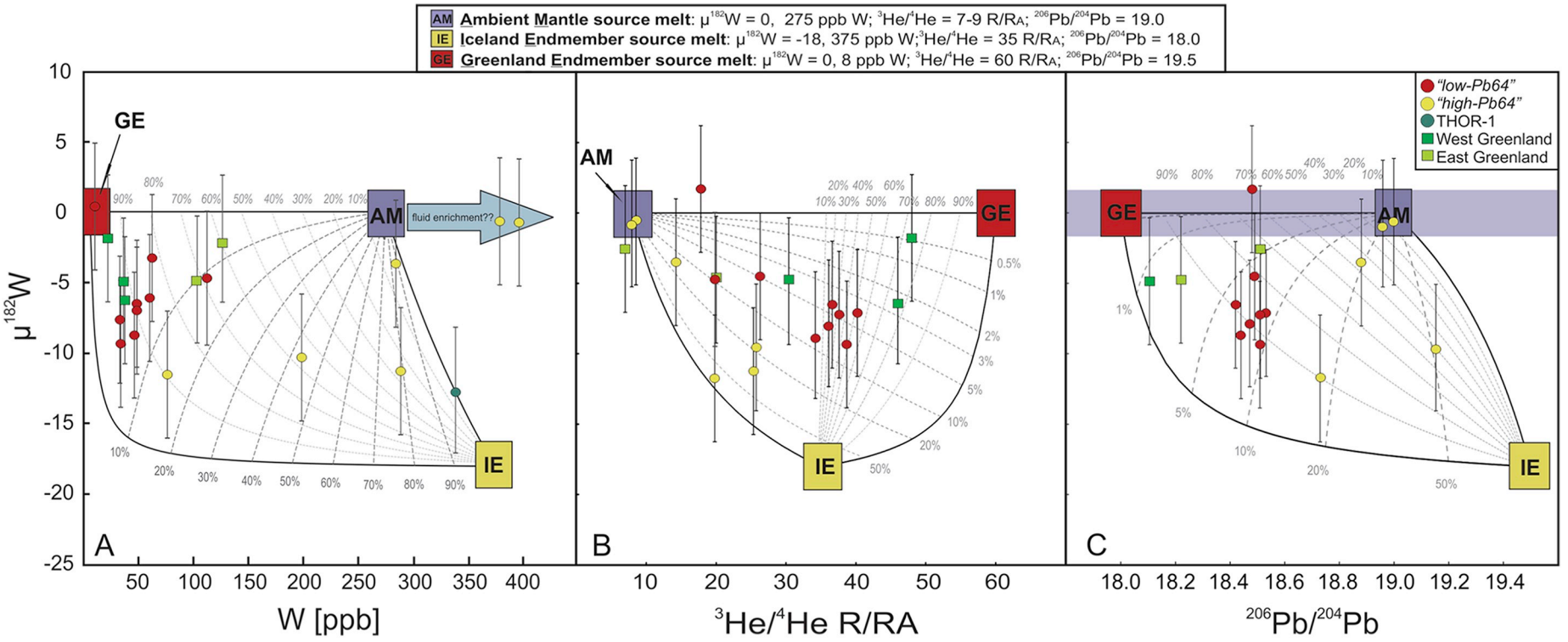

Fig. 5. $\mu^{182}W$ versus (A) W concentrations, (B) $^{3}He/^{4}He$, and (C) $^{206}Pb/^{204}Pb$ showing mixing trends of three source reservoir melt components. $^{206}Pb/^{204}Pb$ data used to plot sample TRI-1 is taken from sample TRI-2. Ambient Mantle component - AM: $\mu^{182}W = 0$; 275 ppb W; $^{206}Pb/^{204}Pb = 19.0$; 0.55 ppm Pb; $^{3}He/^{4}He = 7–9$ R/R_A, 2.0×10^{-10} cm^3 STP/g ^{3}He. Iceland Endmember component - IE: $\mu^{182}W = -18$; 375 ppb W; $^{206}Pb/^{204}Pb = 19.5$; 1.5 ppm Pb; $^{3}He/^{4}He = 35$ R/R_A, 6.0×10^{-10} cm^3 STP/g ^{3}He. Greenland Endmember component - GE: $\mu^{182}W = 0$; 8 ppb W; $^{206}Pb/^{204}Pb = 19.5$; 0.3 ppm Pb; $^{3}He/^{4}He = 60$ R/R_A, 4.5×10^{-10} cm^3 STP/g ^{3}He. Error bars as in Fig. 3. Percentages in dark grey represent the proportion of a melt component from a Source 2 – Source 3 mixture which is then mixed with Source 1, represented by dark grey dashed lines. Percentages in light grey and italic are proportions of GE in a GE–AM mixture; light grey dotted lines are respective mixing lines with IE. Samples from Greenland and the "*low-Pb64*" Iceland group are a mixture of mainly the GE (> 90%) and < 10% of IE with up to ~12% ambient mantle material. Samples from the "*high-Pb64*" group show larger mixing variations of all three source components. The two samples plotting outside of the $\mu^{182}W$-W [ppb] mixing field may have experienced W enrichment by fluid addition. Symbols as in Fig. 2.

SNS206 and SNS214) and SIVZ (samples TRI-1, TRI-2) are dominated by more radiogenic Pb isotopic compositions. By contrast, basalts from the Northern Volcanic Zone and Eastern Volcanic Zone (sample A27) are largely characterized by lower Pb isotopic ratios (e.g., Kokfelt et al., 2006). The WRZ (sample ICE-14-32A) and the RP (sample STAP-1) include both "*high*" and "*low*"-$^{206}Pb/^{204}Pb$ basalts. The Pb isotopic variability evident from neovolcanic eruptions may largely be attributed to melting different portions of distinct plume components as a result of gradual upwelling (e.g., Harðardóttir et al., 2018).

The He, W and Pb isotopic compositions of individual samples may be broadly explained by three-component mixing based on models that combine possible melt compositions from three proposed endmember mantle source domains (Fig. 5A–C). As follows, we first define the required He, W and Pb isotopic/chemical compositions of melt endmember compositions that, when mixed in varying proportions, can account for the characteristics observed in the Greenland-Iceland suite. In the following section we speculate on how the compositions of these mantle source domains could have been generated.

The He-W isotopic characteristics of the **ambient mantle** source (**AM**) are indistinguishable from DMM with $\mu^{182}W \sim 0$ and $^{3}He/^{4}He$ 7–9 R/R_A. Despite this similarity, the **AM** source, that may represent a major portion of Earth's mantle, could also include variable contributions from ancient or young subducted slabs, or mixtures thereof. For instance, $^{206}Pb/^{204}Pb$ ratios of mid-Atlantic Ridge samples range from as low as 16.5 to as high as 20.1 (Agranier et al., 2005, and references therein; Fig. 7), while some plume-derived lavas even exceed this range to $^{206}Pb/^{204}Pb$ up to 22 (e.g., Class and Goldstein, 2005). Thus, long-lived radiogenic isotopic compositions of this source domain, including Pb and Os isotopes, may be regionally distinct and characterized by a range of compositions. The proposed primordial **Iceland endmember** source (**IE**), is characterized by enrichment in incompatible trace elements (most notably W) and is minimally to modestly degassed, with high $^{3}He/(Th + U)$ and correspondingly high $^{3}He/^{4}He$ of ≥ 35 R/R_A. Lead isotopic compositions are comparatively high with $^{206}Pb/^{204}Pb$ of 19.5. The negative $\mu^{182}W$ of this source suggests that it involves an isotopic domain that formed during the lifetime of ^{182}Hf, within the first ~60 Ma of SS history. A third source, the primordial **Greenland endmember** (**GE**), is characterized by incompatible element depletion. The highest measured $^{3}He/^{4}He$ of ~50 R/R_A in samples from West Greenland suggests that this source has an even higher $^{3}He/^{4}He$ than **IE**. Consequently, it must be assumed to be minimally degassed. This observation, in combination with its incompatible element depletion would result in high $^{3}He/(Th + U)$. Hence, given the limited radiogenic ^{4}He production within such a mantle domain, the **GE** could retain a high $^{3}He/^{4}He$ until the present. The **GE** is, therefore, posited to be a second primordial mantle domain with $^{3}He/^{4}He$ of 60 R/R_A. In contrast to the **IE**, it is characterized by a relatively low $^{206}Pb/^{204}Pb$ of 18.0 and a comparatively low W concentration. The normal $\mu^{182}W$ indicates that this source formed > 60 Ma into SS history.

Mixing models require knowledge of elemental concentrations of the participating components, yet constraining the concentrations of He, W, and Pb in all three sources is problematic. Elemental concentrations in the sampled igneous products reflect a combination of source concentrations, degrees of partial melting, and subsequent crystal-liquid fractionation processes. Bulk rock major and trace element data of the studied samples (e.g., MgO, Th; Fig. S2) suggest generally lower melt fractions for the "*high-Pb64*" group compared to the "*low-Pb64*" group and the basalts from Greenland. Helium, W and Pb concentrations for the proposed source components in the mixing models are therefore chosen in accordance with bulk rock data, where individual endmember compositions may reflect different degrees of melting in the source, affecting elemental concentrations. The objective here is to produce a plausible model for producing basalts with the observed isotopic and chemical characteristics, rather than finding a unique solution.

For modeling purposes here, accurately estimating the relative proportions of He, W and Pb in the projected endmember mantle sources is more important than defining absolute He, W and Pb source concentrations. Here, these proportions were chosen based on the proposed degassing histories and source formation processes. As a result of the highly incompatible behavior of W in the silicate system, small melt fractions of an incompatible element enriched source would

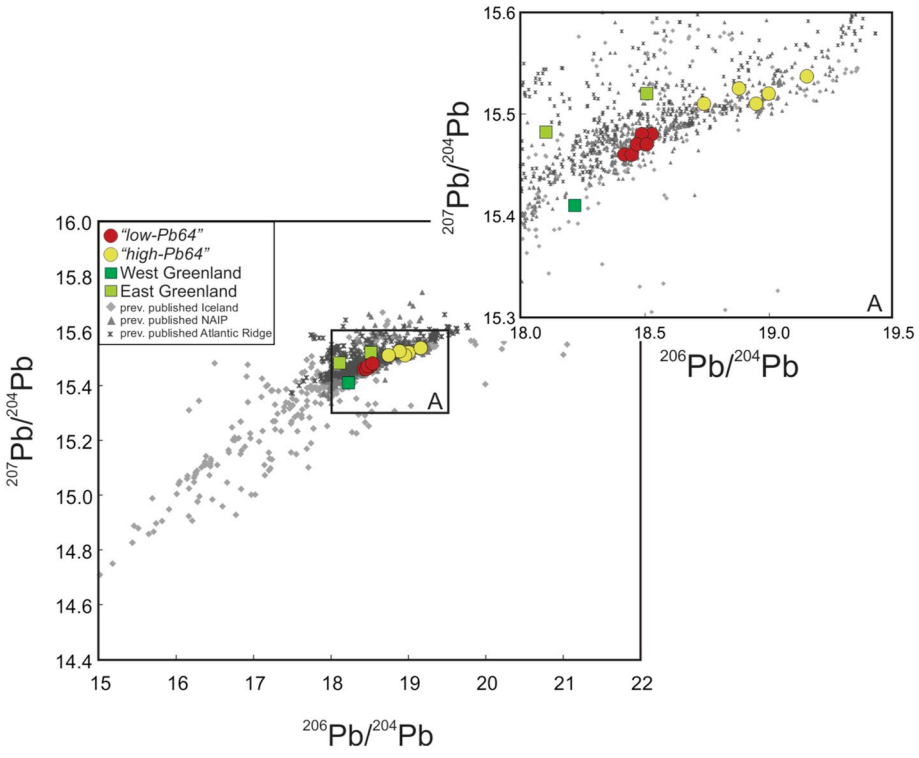

Fig. 6. $^{206}Pb/^{204}Pb$ versus $^{207}Pb/^{204}Pb$. Samples from this study plot within the field of previously published data from the NAIP, Iceland and Atlantic Ridge. Previously published NAIP and Iceland data from the Georoc database (http://georoc.mpch-mainz.gwdg.de/georoc); Atlantic Ridge sample data from Agranier et al. (2005), and references therein.

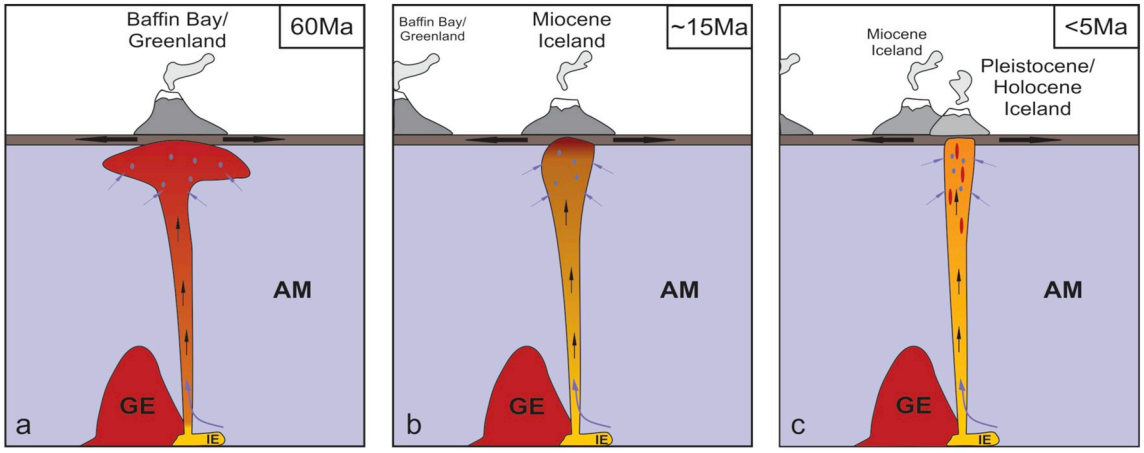

Fig. 7. Simplified cartoon of the proposed evolution of the Iceland plume necessary to account for the observed variations in Pb-He-W isotopic compositions. Left panel (A): The head of the plume carries mostly **GE** material (indicated by the same red color) leading to normal $\mu^{182}W$ signatures and very high $^{3}He/^{4}He$ in Greenland samples that erupted ca. 60 Ma ago. Middle panel (B): During the mid-Miocene, the plume head material becomes diluted by an **IE** tail component that taps a different deep-seated primordial mantle reservoir. This changes the ^{182}W isotopic composition to a more negative value. Right panel (C): In the Pleistocene and Holocene, the proportions of the **IE** and **GE** components in the mantle plume episodically change leading to the observed resolved negative ^{182}W signatures of the "*high-Pb64*" sample group and a "normal" $\mu^{182}W$ in combination with elevated $^{3}He/^{4}He$ in Holocene sample ICE-14-32A from the WRZ. At all stages, the surrounding ambient mantle material (**AM**) is entrained into and mixed with the mantle plume leading to the observed correlation of $\mu^{182}W$ and $^{3}He/^{4}He$. (For interpretation of the references to color in this figure legend, the reader is referred to the web version of this article.)

be characterized by relatively high W and He concentrations. Thus, melt component concentrations will reflect the source composition in combination with source melt fractions. The melt from the **AM** component is assumed to have a normal $\mu^{182}W$ value of 0 and W concentration of 275 ppb, a $^{3}He/^{4}He$ of 8 R/R_A and ^{3}He concentration of 2.0×10^{-10} cm^3STP/g which reflects the degassed nature of this source. It is also assumed to have a $^{206}Pb/^{204}Pb$ of 19.0, which is within the range of Atlantic MORB (Fig. 6), and Pb concentration of 0.55 ppm. These parameters are appropriate for derivation from low melt fractions of the **AM** component with isotopic and chemical compositions very similar to the DMM. A second component is melt from the **IE** that likely results from low degrees of melting of a minimally degassed primordial mantle source and is thus characterized by a projected $\mu^{182}W$ value of −18 (exceeding the lowest measured $\mu^{182}W$ of -12.9 ± 4.5) and 375 ppb W, and a $^{3}He/^{4}He$ of 35 R/R_A and ^{3}He concentration of 6.0×10^{-10} cm^3STP/g, distinctly higher than the **AM** component. It is also assumed to have a $^{206}Pb/^{204}Pb$ of 19.5 and Pb concentration of 1.5 ppm. The third component is melt from the **GE**, which is characterized by a $\mu^{182}W$ of 0 and, because the source for this melt component is assumed to be a minimally degassed incompatible element depleted mantle domain and has experienced high degrees of melting, a low W concentration of 8 ppb, a $^{3}He/^{4}He$ of 60 R/R_A and ^{3}He concentration of 4.5×10^{-10} cm^3STP/g, and $^{206}Pb/^{204}Pb$ of 18.0 and a Pb concentration of 0.3 ppm.

By design, the mixing curves between the three endmember melt components encompass the Pb-He-W isotopic data for all samples (Fig. 5A–C). Thus, mixing between these hypothesized endmember compositions can account for all observed He, W and Pb isotopic compositions observed. The three apparent He-W trends for the Greenland samples and "*high-Pb64*" and "*lowPb64*" samples suggest that each trend may reflect two component mixing between **AM** and a discrete source composition within the three endmember component field characterized by high $^{3}He/^{4}He$, and normal, slightly negative and more highly negative $\mu^{182}W$ values. The mixing models suggest that the "*low-Pb64*" group samples, as well as the Paleocene samples from Greenland, are composed mainly of **GE** melts, characterized by normal $\mu^{182}W$, low W concentrations, high $^{3}He/^{4}He$, and relatively low $^{206}Pb/^{204}Pb$. By contrast, the **IE** is the main primordial source component for the "*high-Pb64*" group samples. While some samples of both the "*high-Pb64*" and the "*low-Pb64*" groups, and samples from Greenland, must have been modified by the addition of **AM** material, mixing calculations suggest a larger proportion of **AM** component in some of the "*high-Pb64*" group samples.

Despite the fact that the observed shallow He-W trend defined by the "*low-Pb64*" group samples requires some addition of **AM** material, the low W concentrations of these samples argue against significant (> 15%) addition of an ambient mantle component (Fig. 5A). Sample ICE-14-32A, which is part of the "*low-Pb64*" group (Fig. 3), has a normal $\mu^{182}W$ value. This isotopic signature may reflect 100% of the "*low-Pb64*" endmember source, without the addition of significant amounts of the "*high-Pb64*" or ambient mantle material. One argument in favor of this interpretation is the low W concentration of ~10 ppb of this sample (Mundl et al., 2017 and this study), which indicates lack of any further addition of mantle melt that would likely be characterized by significantly higher W concentrations. However, the moderate $^{3}He/^{4}He$ of 17 R/R_A suggests the addition of a third, low-$^{3}He/^{4}He$ component with low W concentrations resulting in the observed lowered $^{3}He/^{4}He$, in comparison to the remaining *low-Pb64* samples with $^{3}He/^{4}He$ of up to 41 R/R_A.

Generally, higher W concentrations in the "*high-Pb64*" group are accompanied by overall higher abundances of similarly incompatible trace elements, such as Th (Fig. S2) indicating lower degrees of partial melting of the source reservoir. Two samples from the SNVZ (SNS206 and SNS214) that plot outside the $\mu^{182}W$ vs. W [ppb] mixing field (Fig. 5A) also plot significantly off the W-Th trend, having distinctly higher W concentrations. These samples are also characterized by elevated concentrations of Ba (Debaille et al., 2009), which may suggest secondary addition of fluid mobile elements (including W, which is highly fluid mobile; König et al., 2008) resulting in the observed high W concentrations.

5.2. Implications for the formation of primordial source reservoirs

Based on noble gas isotopic compositions (He, Ne, and Xe), several prior studies have concluded that the Iceland plume taps a primordial, ancient mantle source domain (e.g., Dixon et al., 2000; Moreira et al., 2001; Starkey et al., 2009; Mukhopadhyay, 2012; Harðardóttir et al., 2018). Consistent with this and based on positive $\mu^{182}W$ values in combination with high $^{3}He/^{4}He$, Rizo et al. (2016a) inferred a contribution from a mantle source domain for Paleocene picrites from the

spatially associated Baffin Bay region of the NAIP that formed within the first 60 Ma of SS history. This may have bearing on the interpretation of the Iceland ^{182}W and $^{3}He/^{4}He$ data as it has been proposed that the Baffin Bay basalts/picrites, as well as the basaltic rocks from West and East Greenland analyzed here, represent the products of the initial stage of melting of the same plume that eventually produced the Iceland basaltic rocks (e.g., Storey et al., 1998).

The negatively sloping $^{3}He/^{4}He$ versus $\mu^{182}W$ trend characteristic of the "*high-Pb64*" Iceland lavas is indistinguishable from the trends defined by lavas from Samoa and Hawaii (Fig. 3: Mundl et al., 2017). This may suggest that the "*high-Pb64*" Iceland trend formed by mixing between an ambient upper mantle melt with low $^{3}He/^{4}He$ and "normal" $\mu^{182}W$ (**AM**), and a melt of an analogous, isotopically anomalous source domain (**IE**) in similar proportions to Hawaii and Samoa. Mundl et al. (2017) considered several processes to account for the creation of the high-$^{3}He/^{4}He$ and low-$\mu^{182}W$ source domain posited for Hawaii and Samoa. These processes include silicate crystal-liquid fractionation and metal-silicate segregation during the lifetime of ^{182}Hf (~60 Ma), as well as core-mantle interaction at any time during Earth history. Of these, explanations calling on silicate crystal-liquid fractionation and direct core-mantle interaction are problematic. In the case of silicate crystal-liquid fractionation, such as may have occurred in a magma ocean, there is no accompanying depletion in ^{142}Nd (Horan et al., 2018). A correlation would be expected because the relative partitioning behaviors of Sm/Nd and Hf/W are broadly similar during high pressure silicate fractionation (Righter and Shearer, 2003). In the case of direct core contamination of a rising plume, neither the Samoan nor the Hawaiian lavas appear to be derived from HSE-enriched sources, as would be expected for even a small contribution from core metal (Mundl et al., 2017). The "normal" HSE abundances in these basalts also obviate the possibility of the involvement of late accreted metals stranded in the mantle, as such metals likely would also be strongly enriched in HSE.

Mundl et al. (2017) further considered metal-silicate interactions during which negative $\mu^{182}W$ derives from a mantle domain that contains primordial metal formed by disproportionation reactions in an early magma ocean. Metal formed by an indigenous process would presumably concentrate W and HSE from surrounding silicates. This metal would have very low Hf/W ratios due to the lithophile and siderophile behaviors of Hf and W, respectively. Given the low Hf/W anticipated for the metal (rendering any subsequent radiogenic ingrowth negligible), the $\mu^{182}W$ of the newly-formed metal would remain constant thereafter, even if the metal formed while ^{182}Hf was still alive. Because of the presumably low concentrations of HSE in the surrounding mantle resulting from prior metal segregation during core formation, the concentrations of the HSE incorporated by the metal would also likely be low. Testing this process is difficult because of the large uncertainties involved in predicting the ^{182}W isotopic composition and W concentration that would be incorporated in the metal, as well as estimating the He concentration in the metal and surrounding silicates.

The conclusions presented by Mundl et al. (2017) regarding the isotopically anomalous component in the Hawaiian and Samoan mixing trends can largely also be applied to the isotopically anomalous **IE** component in the Icelandic "*high-Pb64*" group. As with Hawaii and Samoa, there is no evidence for variations in ^{142}Nd in Icelandic lavas (Andreasen et al., 2008; Murphy et al., 2010), so there is no supporting evidence for early silicate crystal-liquid fractionation processes. Similarly, HSE abundances are not anomalously high in the "*high-Pb64*" lavas, eliminating direct core contamination of the plume as a possible explanation for a negative $\mu^{182}W$ source.

It is possible that subducted Archean crust accumulated at the core-mantle boundary (CMB) or at the mantle transition zone, and contributed material to the Hawaiian and Samoan plumes. The presence of Archean rocks with both positive and negative $\mu^{182}W$ values are now well documented (e.g., Willbold et al., 2011; Touboul et al., 2012, 2014; Liu et al., 2016a, 2016b; Rizo et al., 2016b; Puchtel et al., 2016, 2018; Reimink et al., 2018; Mundl et al., 2018; Tusch et al., 2019), and hence, could be contributors to mantle-derived systems with both negative and positive $\mu^{182}W$. Subducted crust, however, would likely be strongly degassed and characterized by low $^{3}He/^{4}He$, so there would be no a priori reason to predict a negative correlation between $\mu^{182}W$ and $^{3}He/^{4}He$ resulting from this scenario.

A final possibility to be considered is chemical (including isotopic) equilibration between the core and lowermost mantle. Based on mass balance considerations, Earth's core is presumed to have a $\mu^{182}W$ value of ~ −220 and a high W concentration of 450 ppb (McDonough, 2003; Kleine and Walker, 2017), reflecting primary core formation within the first 30 Ma of SS history. Equilibration between the core and a portion of the mantle may have been efficient during the lifetime of one or more basal magma ocean events. Thus, a plume rising from the CMB may receive a contribution from the remnants of a core-equilibrated basal magma ocean at any time in Earth history. The concentration of He in the core is poorly constrained (e.g., Matsuda et al., 1993; Bouhifd et al., 2013), so it is not currently possible to predict the effect core-mantle equilibration might have on the isotopic composition of He on a melted region at the core-mantle boundary. Regardless, the addition of core He to the plume source is not necessary for this model. The He contained within the remnant portion of a basal magma ocean would likely be primordial and harbor high $^{3}He/^{4}He$. Similarly, the HSE concentrations in the remnant domain would accord with high-temperature and -pressure metal-silicate exchange (e.g., Mann et al., 2012), and hence, would not be expected to contain anomalously high or low concentrations of these elements. Overall, the projected characteristics of such a reservoir could match the envisioned characteristics of the **IE**.

Possibly the best candidates for the remnants of a basal magma ocean are seismically identified ultra-low velocity zones (ULVZ; e.g., Labrosse et al., 2007). Ultra-low velocity zones are volumetrically small features and it has been speculated that they consist of dense, Fe-rich melt, or that they may even contain metallic Fe (Mao et al., 2006; Wicks et al., 2010; Liu et al., 2016a, 2016b). A dense silicate melt, a potential remnant from an early-formed magma ocean trapped at the CMB could be enriched in incompatible elements, such as Th and U. Over time this would lead to significant production of ^{4}He (a radiogenic product from the decay of Th and U), lowering the $^{3}He/^{4}He$ over time. Nevertheless, because this deep-seated mantle domain could remain minimally degassed, initial high ^{3}He abundances, and consequently comparatively high $^{3}He/^{4}He$ due to high $^{3}He/(U + Th)$, would be retained. Thus, despite the production of radiogenic ^{4}He over a period of 4.5 Ga, the $^{3}He/^{4}He$ today could remain significantly higher than that of MORB. Ultra-low velocity zones constitute a particularly attractive option for the location of the isotopically anomalous endmember of the Hawaiian, Samoan, and now the "*high-Pb64*" Icelandic trends, as French and Romanowicz (2015) and Yuan and Romanowicz (2017) have seismically identified ULVZs beneath all three hotspots.

The new $\mu^{182}W$ values in combination with previously published $^{3}He/^{4}He$ of up to 48 R/RA for the East and West Greenland samples studied here, require at least one additional primordial source reservoir associated with the Iceland plume. This source (**GE**) is characterized by modern upper mantle-like $\mu^{182}W = 0$, but high $^{3}He/^{4}He$. The high $^{3}He/^{4}He$ indicates that it must have formed early in Earth's history and subsequently remained unaffected by material recycling until at least recent times. If the normal $\mu^{182}W$ values are representative of the mantle source domain revealed by the "*Greenland*" trend, it may indicate formation of a second primordial domain after ^{182}Hf became extinct (~60 Ma following SS formation). Based on Pb isotope compositions in lavas from Baffin Island and West Greenland, Jackson et al. (2010) argued for a 4.5 Ga year old origin of the $^{3}He/^{4}He$ mantle source tapped by the proto-Iceland mantle plume. Distinctly higher $^{3}He/^{4}He$ than those characterizing the **IE** may indicate higher initial He/(Th + U) ratios. Rizo et al. (2016a) suggested a seismically anomalous mantle domain as source for the Baffin Bay flood basalts, the stratigraphic equivalents to the West Greenland samples examined here. So-called large low shear velocity provinces (LLSVP) have been interpreted

to represent deep un-degassed mantle reservoirs (e.g. Labrosse et al., 2007) and, thus, may be a potential candidate for the **GE**. Alternatively, Ballmer et al. (2016) suggested that primordial mantle domains representing the first crystallization products of an ancient magma ocean may be stored as "bridgmanite-enriched ancient mantle structures" (BEAMS) in the deep mantle. These early-formed domains may become eroded over time and, thus, in some regions, may be tapped by ancient and recent mantle plumes. Hence, these mantle structures could also represent a **GE** component manifested in the geochemical signature of the presumed head of the Iceland mantle plume.

The first crystallized domains of an early magma ocean that formed > 60 Ma into SS history would be characterized by a high Hf/W ratio resulting from the more highly incompatible behavior of W relative to Hf (e.g., Righter and Shearer, 2003). Because ^{182}Hf would be extinct by then, the μ^{182}W of this mantle domain would remain constant, resulting in μ^{182}W signatures indistinguishable from modern upper mantle values. Additionally, as this source would be expected to have low overall incompatible trace element abundances, the presumed primordial, minimally degassed mantle section should also be characterized by a high He/(Th + U) ratio, assuming a higher incompatibility of He relative to Th and U (Parman et al., 2005). Consequently, lesser amounts of radiogenic ^{4}He than in a source with a lower He/(Th + U) ratio (**IE**) would be produced, and, thus, retaining higher ^{3}He/^{4}He over 4.5 Ga in the **GE** compared to the **IE**. Similarly, the higher compatibility of Pb relative to U and Th would result in a (Th + U)/Pb ratio of a residual melt (**IE**) that is higher than that of a reservoir enriched in compatible elements (**GE**). Consequently, because less radiogenic Pb is produced in this incompatible element (Th and U) depleted **GE**, it would evolve towards lower ^{206}Pb/^{204}Pb over time compared to the **IE**. This compatible element enriched mantle domain would also be expected to be characterized by higher concentrations of HSE, especially the more refractory IPGE, compared to an incompatible element enriched melt layer. This is consistent with HSE concentrations determined for the "*low-Pb64*" and the "*high-Pb64*" groups (Table 2, Fig. 4).

Assuming the existence of a mantle domain with normal μ^{182}W but high ^{3}He/^{4}He, the "*low-Pb64*" trend could reflect mixtures of materials between the initial horizontal trend defined by the East and West Greenland basalts, and the "*high-Pb64*" trend. This possibility is considered in the next section.

5.3. Geochemical evolution of the NAIP mantle plume

It has previously been recognized (e.g., Forsyth et al., 1986; Storey et al., 1998) that there is a connection between the Iceland hotspot and the mantle plume that led to the Tertiary NAIP. The Paleocene basalts from Baffin Bay and West Greenland have been interpreted to represent the initial phase of the mantle plume that remains active today under Iceland (e.g., Starkey et al., 2009; Graham et al., 1998). Volcanic successions that are several km thick are suggested to reflect the high-temperature melting of the plume head (Holm et al., 1993; Gill et al., 1995). The head of this mantle plume, that erupted ca. 60 Ma ago, could have primarily consisted of mainly the **GE** mantle material characterized by normal μ^{182}W and high ^{3}He/^{4}He (Fig. 7A). During the Miocene, the composition of the mantle plume is projected to have changed such that, in addition to the **GE**, **IE** material was also tapped (Fig. 7B). As time progressed, the Pleistocene and Holocene eruptions within the current neovolcanic zones of Iceland might have been derived from the mantle plume tail that mainly tapped an **IE** component (Fig. 7C). According to the mixing model, the mantle plume in all three scenarios also incorporated various amounts of ambient mantle material (**AM**; Figs. 4, 7). Jones et al. (2019) recently showed that heads of mantle plumes may sample different deep-seated mantle sources than plume tails resulting in compositional changes of plume material with time. In agreement with their geodynamical model, the present study provides the first geochemical evidence for temporal evolution of a single mantle plume reflected primarily in its short-lived radiogenic isotope composition.

Rizo et al. (2016a) reported positive μ^{182}W values in combination with high ^{3}He/^{4}He for Baffin Bay basalts. Given the suggestion that the Baffin Bay samples studied by Rizo et al. (2016a) and the West Greenland basalts studied here are stratigraphically similar (Starkey et al., 2009), the positive ^{182}W signatures observed in Baffin Bay versus the "normal" ^{182}W of West Greenland basalts suggest either a third primordial source reservoir accessed by the plume, or require an alternative explanation for the positive ^{182}W values in the samples from Baffin Bay, such as a small contribution of W-rich Archean continental crust, which is abundant in the area (Lightfoot et al., 1997). Because of the very low W concentrations of samples from Baffin Bay and West Greenland, mixing calculations show that as little as 3% of a crustal component with relatively high W concentrations, characterized by a μ^{182}W of +15, would be sufficient to change the μ^{182}W value from 0 to +10 (Fig. S8). Thus, the number of different primordial source reservoirs remains unclear at this time.

6. Conclusions

The He-W data for products of the Greenland-Iceland plume require the presence of at least two primordial mantle domains, characterized by distinct isotopic signatures that have been preserved in Earth's mantle and are accessible to mantle plumes today. Icelandic basalt samples are characterized by negative μ^{182}W values as low as -12.9 ± 4.5 ppm. These signatures correlate with ^{3}He/^{4}He and, based on Pb isotope compositions, samples from Iceland form two distinct He-W trends resulting from the mixing of two separate primordial mantle sources with an ambient mantle melt component. While samples with negative μ^{182}W values require a source that formed during the lifetime of ^{182}Hf and potentially represents a remnant of a magma ocean that equilibrated with the core, the "normal" ^{182}W signatures of East and West Greenland samples together with ^{3}He/^{4}He of up to 48 R/R_A suggest an additional primordial mantle source that formed after ^{182}Hf was no longer extant.

The chemical evolution from the initial phase of the mantle plume (i.e., East and West Greenland flood basalts) to the present-day (Iceland), which is manifested in distinct ^{182}W and ^{3}He/^{4}He characteristics of the eruption products, suggests that the composition of the mantle plume changed episodically with time, with the head of the NAIP plume tapping a different primordial source reservoir than its tail. More recent variations in source component proportions may further be attributed to changes in the geometry of the plume melting regions of this tectonically complex system.

Acknowledgements

This study was supported by NSF grant EAR-1624587 (to RJW and AMP). AMP acknowledges FWF grant V659-N29. MJ acknowledges NSF grant EAR-1624840, and MK acknowledges OCE-1259218. We would like to thank Lotte M. Larsen and Asger K. Pedersen for providing the West Greenland samples, and Bernard Marty for the samples from East Greenland. We thank Catherine Chauvel for the editorial handling and Rita Parai, Dominique Weis, David Graham and an anonymous reviewer for the helpful and constructive comments on this and an earlier version of the manuscript.

Appendix A. Supplementary data

Supplementary data to this article can be found online at https://doi.org/10.1016/j.chemgeo.2019.07.026.

References

Agranier, A., Blichert-Toft, J., Graham, D., Debaille, V., Schiano, P., Albarède, F., 2005. The spectra of isotopic heterogeneities along the mid-Atlantic Ridge. Earth Planet. Sci. Lett. 238, 96–109. https://doi.org/10.1016/j.epsl.2005.07.011.

Agranier, A., Maury, R.C., Geoffroy, L., Chauvet, F., Le Gall, B., Viana, A.R., 2019. Volcanic record of continental thinning in Baffin Bay margins: insights from Svartenhuk Halvø Peninsula basalts, West Greenland. Lithos 334–335, 117–140. https://doi.org/10.1016/j.lithos.2019.03.017.

Albarède, F., Telouk, P., Blichert-Toft, J., Boyet, M., Agranier, A., Nelson, B., 2004. Precise and accurate isotopic measurements using multiple-collector ICPMS. Geochim. Cosmochim. Acta 68, 2725–2744. https://doi.org/10.1016/j.gca.2003.11.024.

Andreasen, R., Sharma, M., Subbarao, K.V., Viladkar, S.G., 2008. Where on Earth is the enriched Hadean reservoir? Earth Planet. Sci. Lett. 266, 14–28. https://doi.org/10.1016/j.epsl.2007.10.009.

Archer, G.J., Mundl, A., Walker, R.J., Worsham, E.A., Bermingham, K.R., 2017. High-precision analysis of $^{182}W/^{184}W$ and $^{183}W/^{184}W$ by negative thermal ionization mass spectrometry: per-integration oxide corrections using measured $^{18}O/^{16}O$. Int. Journ. Mass Spectr. 414, 80–86. https://doi.org/10.1016/j.ijms.2017.01.002.

Ballmer, M.D., Schumacher, L., Lekic, V., Thomas, C., Ito, G., 2016. Compositional layering within the large low shear-wave velocity provinces in the lower mantle. Geochem. Geophy. Geosy. 17, 5056–5077. https://doi.org/10.1002/2016GC006605.

Becker, H., Horan, M.F., Walker, R.J., Gao, S., Lorand, J.P., Rudnick, R.L., 2006. Highly siderophile element composition of the Earth's primitive upper mantle: Constraints from new data on peridotite massifs and xenoliths. Geochim. Cosmochim. Acta 70, 4528–4550. https://doi.org/10.1016/j.gca.2006.06.004.

Birck, J.L., Barman, M.R., Capmas, F., 1997. Re-Os isotopic measurements at the femtomole level in natural samples. Geostand. Newslett. 21, 19–27. https://doi.org/10.1111/j.1751-908X.1997.tb00528.x.

Bouhifd, M.A., Jephcoat, A.P., Heber, V.S., Kelley, S.P., 2013. Helium in Earth's early core. Nat. Geosc. 6, 982–986.

Brandon, A.D., Graham, D.W., Waight, T., Gautason, B., 2007. ^{186}Os and ^{187}Os enrichments and high-$^{3}He/^{4}He$ sources in the Earth's mantle: evidence from Icelandic picrites. Geochim. Cosmochim. Acta 71, 4570–4591. https://doi.org/10.1016/j.gca.2007.07.015.

Breddam, K., Kurz, M.D., Storey, M., 2000. Mapping out the conduit of the Iceland mantle plume with helium isotopes. Earth Planet. Sci. Lett. 176, 45–55. https://doi.org/10.1016/S0012-821X(99)00313-1.

Burnard, P., Harrison, D., 2005. Argon isotope constraints on modification of oxygen isotopes in Iceland Basalts by surficial processes. Chem. Geol. 216, 143–156. https://doi.org/10.1016/j.chemgeo.2004.11.001.

Chauvel, C., Hémond, C., 2000. Melting of a complete section of recycled oceanic crust: trace element and Pb isotopic evidence from Iceland. Geochemi. Geophys. Geosys. 1. https://doi.org/10.1029/1999GC000002.

Class, C., Goldstein, S.L., 2005. Evolution of helium isotopes in the Earth's mantle. Nature 436, 1107–1112. https://doi.org/10.1038/nature03930.

Cohen, A.S., Waters, F.G., 1996. Separation of osmium from geological materials by solvent extraction for analysis by thermal ionisation mass spectrometry. Analyt. Chim. Acta 332, 269–275. https://doi.org/10.1016/0003-2670(96)00226-7.

Dale, C.W., Pearson, D.G., Starkey, N.A., Stuart, F.M., Ellam, R.M., Larsen, L.M., Fitton, J.G., Macpherson, C.G., 2009. Osmium isotopes in Baffin Island and West Greenland picrites: implications for the $^{187}Os/^{188}Os$ composition of the convecting mantle and the nature of high 3He/4He mantle. Earth Planet. Sci. Lett. 278, 267–277. https://doi.org/10.1016/j.epsl.2008.12.014.

Dale, C.W., Kruijer, T.S., Burton, K.W., 2017. Highly siderophile element and ^{182}W evidence for a partial late veneer in the source of 3.8 Ga rocks from Isua, Greenland. Earth Planet. Sci. Lett. 458, 394–404. https://doi.org/10.1016/j.epsl.2016.11.001.

Debaille, V., Trønnes, R.G., Brandon, A.D., Waight, T.E., Graham, D.W., Lee, C.-T.A., 2009. Primitive off-rift basalts from Iceland and Jan Mayen: Os-isotopic evidence for a mantle source containing enriched subcontinental lithosphere. Geochim. Cosmochim. Acta 73, 3423–3449. https://doi.org/10.1016/j.gca.2009.03.002.

Dixon, E.T., Honda, M., McDougall, I., Campbell, I.H., Sigurdsson, I., 2000. Preservation of near-solar neon isotopic ratios in Icelandic basalts. Earth Planet. Sci. Lett. 180, 309–324. https://doi.org/10.1016/S0012-821X(00)00164-3.

Eisele, J., Abouchami, W., Galer, S.J.G., Hofmann, A.W., 2003. The 320 kyr Pb isotope evolution of Mauna Kea lavas recorded in the HSDP-2 drill core. Geochem. Geophys. Geosys. 4. https://doi.org/10.1029/2002GC000339.

Ellam, R.M., Upton, B.G.J., Fitton, J.G., 1998. Petrogenesis of late stage magmatism at hold with Hope, East Greenland. Contrib. Min. Petr. 133, 51–59. https://doi.org/10.1007/s004100050436.

Forsyth, D., Morel-A-L'Huissier, P., Asudeh, I., Green, A., 1986. Alpha Ridge and Iceland-products of the same plume? J. Geodyn. 6, 197–214. https://doi.org/10.1016/0264-3707(86)90039-6.

French, S.W., Romanowicz, B., 2015. Broad plumes rooted at the base of the Earth's mantle beneath major hotspots. Nature 525, 95.

Füri, E., Hilton, D.R., Halldórsson, S.A., Barry, P.H., Hahm, D., Fischer, T.P., Grönvold, K., 2010. Apparent decoupling of the He and Ne isotope systematics of the Icelandic mantle: the role of He depletion, melt mixing, degassing fractionation and air interaction. Geochim. Cosmochim. Acta 74, 3307–3332. https://doi.org/10.1016/j.gca.2010.03.023.

Gill, R.C.O., Holm, P.M., Nielsen, T.F.D., 1995. Was a short-lived Baffin Bay plume active prior to initiation of the present Icelandic plume? Clues from the high-Mg picrites of West Greenland. Lithos 34, 27–39. https://doi.org/10.1016/0024-4937(95)90007-1.

Graham, D.W., 2002. Noble gas isotope geochemistry of mid-ocean ridge and ocean island basalts: characterization of mantle source reservoirs. Rev. Min. Geochem. 47, 247–317. https://doi.org/10.2138/rmg.2002.47.8.

Graham, D.W., Larsen, L.M., Hanan, B.B., Storey, M., Pedersen, A.K., Lupton, J.E., 1998. Helium isotope composition of the early Iceland mantle plume inferred from the Tertiary picrites of West Greenland. Earth Planet. Sci. Lett. 160, 241–255. https://doi.org/10.1016/S0012-821X(98)00083-1.

Halldórsson, S.A., Barnes, J.D., Stefánsson, Andri, Hilton, D.R., Hauri, E.H., Marshall, Edward W., 2016a. Subducted lithosphere controls halogen enrichments in the Iceland mantle plume source. Geology 44, 679–682. https://doi.org/10.1130/G37924.1.

Halldórsson, S.A., Hilton, D.R., Barry, P.H., Füri, E., Grönvold, K., 2016. Recycling of crustal material by the Iceland mantle plume: new evidence from nitrogen elemental and isotope systematics of subglacial basalts. Geochim. Cosmochim. Acta 176, 206–226. https://doi.org/10.1016/j.gca.2015.12.021.

Hanan, B.B., Schilling, J.-G., 1997. The dynamic evolution of the Iceland mantle plume: the lead isotope perspective. Earth Planet. Sci. Lett. 151, 43–60. https://doi.org/10.1016/S0012-821X(97)00105-2.

Hanan, B.B., Blichert-Toft, J., Kingsley, R., Schilling, J.-G., 2000. Depleted Iceland mantle plume geochemical signature: Artifact of multicomponent mixing? Geochem. Geophys. Geosyst. 1. https://doi.org/10.1029/1999GC000009.

Harðardóttir, S., Halldórsson, S.A., Hilton, D.R., 2018. Spatial distribution of helium isotopes in Icelandic geothermal fluids and volcanic materials with implications for location, upwelling and evolution of the Icelandic mantle plume. Chem. Geol. 480, 12–27. https://doi.org/10.1016/j.chemgeo.2017.05.012.

Hemond, C., Arndt, N.T., Lichtenstein, U., Hofmann, A.W., Oskarsson, N., Steinthorsson, S., 1993. The heterogeneous Iceland plume: Nd-Sr-O isotopes and trace element constraints. Journ. Geophys. Res.: Solid Earth 98, 15833–15850. https://doi.org/10.1029/93JB01093.

Holm, P.M., Gill, R.C.O., Pedersen, A.K., Larsen, J.G., Hald, N., Nielsen, T.F.D., Thirlwall, M.F., 1993. The Tertiary picrites of West Greenland: contributions from 'Icelandic' and other sources. Earth Planet. Sci. Lett. 115, 227–244. https://doi.org/10.1016/0012-821X(93)90224-W.

Horan, M.F., Carlson, R.W., Walker, R.J., Jackson, M., Garçon, M., Norman, M., 2018. Tracking Hadean processes in modern basalts with 142-Neodymium. Earth Planet. Sci. Lett. 484, 184–191. https://doi.org/10.1016/j.epsl.2017.12.017.

Jackson, M.G., Carlson, R.W., Kurz, M.D., Kempton, P.D., Francis, D., Blusztajn, J., 2010. Evidence for the survival of the oldest terrestrial mantle reservoir. Nature 466, 853.

Jones, T.D., Davies, D.R., Sossi, P.A., 2019. Tungsten isotopes in mantle plumes: heads it's positive, tails it's negative. Earth Planet. Sci. Lett. 506, 255–267. https://doi.org/10.1016/j.epsl.2018.11.008.

Kerr, A.C., Saunders, A.D., Tarney, J., Berry, N.H., Hards, V.L., 1995. Depleted mantle-plume geochemical signatures: no paradox for plume theories. Geology 23, 843–846. https://doi.org/10.1130/0091-7613(1995)023<0843:DMPGSN>2.3.CO;2.

Kleine, T., Walker, R.J., 2017. Tungsten Isotopes in Planets. Annu. Rev. Earth Planet. Sci. 45, 389–417. https://doi.org/10.1146/annurev-earth-063016-020037.

Kleine, T., Mezger, K., Münker, C., Palme, H., Bischoff, A., 2004. ^{182}Hf-^{182}W isotope systematics of chondrites, eucrites, and martian meteorites: chronology of core formation and early mantle differentiation in Vesta and Mars. Geochim. Cosmochim. Acta 68, 2935–2946. https://doi.org/10.1016/j.gca.2004.01.009.

Kokfelt, T.F., Hoernle, K., Hauff, F., Fiebig, J., Werner, R., Garbe-Schönberg, D., 2006. Combined trace element and Pb-Nd–Sr-O isotope evidence for recycled oceanic crust (upper and lower) in the Iceland Mantle Plume. J. Pet. 47, 1705–1749. https://doi.org/10.1093/petrology/egl025.

König, S., Münker, C., Schuth, S., Garbe-Schönberg, D., 2008. Mobility of tungsten in subduction zones. Earth Planet. Sci. Lett. 274, 82–92. https://doi.org/10.1016/j.epsl.2008.07.002.

Kruijer, T.S., Kleine, T., 2018. No 182W excess in the Ontong Java Plateau source. Chem. Geol. 485, 24–31. https://doi.org/10.1016/j.chemgeo.2018.03.024.

Kurz, M.D., Curtice, J., Lott III, D.E., Solow, A., 2004. Rapid helium isotopic variability in Mauna Kea shield lavas from the Hawaiian Scientific Drilling Project. Geochem. Geophys. Geosys. 5. https://doi.org/10.1029/2002GC000439.

Labrosse, S., Hernlund, J.W., Coltice, N., 2007. A crystallizing dense magma ocean at the base of the Earth's mantle. Nature 450, 866. https://doi.org/10.1038/nature06355.

Larsen, L.M., Pedersen, A.K., 2009. Petrology of the Paleocene Picrites and flood basalts on Disko and Nuussuaq, West Greenland. J. Pet. 50, 1667–1711. https://doi.org/10.1093/petrology/egp048.

Lightfoot, P.C., Hawkesworth, C.J., Olshefsky, K., Green, T., Doherty, W., Keays, R.R., 1997. Geochemistry of Tertiary tholeiites and picrites from Qeqertarssuaq (Disko Island) and Nuussuaq, West Greenland with implications for the mineral potential of comagmatic intrusions. Contr. Min. Petr. 128, 139–163. https://doi.org/10.1007/s004100050300.

Liu, Jiachao, Li, J., Hrubiak, R., Smith, J.S., 2016a. Origins of ultralow velocity zones through slab-derived metallic melt. Proc. Natl. Acad. Sci. U. S. A. 113, 5547. https://doi.org/10.1073/pnas.1519540113.

Liu, Jingao, Touboul, M., Ishikawa, A., Walker, R.J., Graham Pearson, D., 2016b. Widespread tungsten isotope anomalies and W mobility in crustal and mantle rocks of the Eoarchean Saglek Block, northern Labrador, Canada: implications for early Earth processes and W recycling. Earth Planet. Sci. Lett. 448, 13–23. https://doi.org/10.1016/j.epsl.2016.05.001.

Mabry, J., Lan, T., Burnard, P., Marty, B., 2013. High-precision helium isotope measurements in air. Journ. Analyt. Atom. Spectr. 28, 1903–1910. https://doi.org/10.1039/C3JA50155H.

Mann, U., Frost, D.J., Rubie, D.C., Becker, H., Audétat, A., 2012. Partitioning of Ru, Rh, Pd, Re, Ir and Pt between liquid metal and silicate at high pressures and high temperatures - implications for the origin of highly siderophile element concentrations in the Earth's mantle. Geochim. Cosmochim. Acta 84, 593–613. https://doi.org/10.

1016/j.gca.2012.01.026.
Mao, W.L., Mao, H., Sturhahn, W., Zhao, J., Prakapenka, V.B., Meng, Y., Shu, J., Fei, Y., Hemley, R.J., 2006. Iron-rich post-perovskite and the origin of ultralow-velocity zones. Science 312, 564. https://doi.org/10.1126/science.1123442.
Marchi, S., Canup, R.M., Walker, R.J., 2018. Heterogeneous delivery of silicate and metal to the Earth by large planetesimals. Nat. Geosci. 11, 77–81. https://doi.org/10.1038/s41561-017-0022-3.
Marty, B., Upton, B.G.J., Ellam, R.M., 1998. Helium isotopes in early Tertiary basalts, northeast Greenland: evidence for 58 Ma plume activity in the North Atlantic–Iceland volcanic province. Geology 26, 407–410. https://doi.org/10.1130/0091-7613(1998)026<0407:HIIETB>2.3.CO;2.
Matsuda, J., Sudo, M., Ozima, M., Ito, K., Ohtaka, O., Ito, E., 1993. Noble gas partitioning between metal and silicate under high pressures. Science 259, 788–790. https://doi.org/10.1126/science.259.5096.788.
McDonough, W.F., 2003. 2.15- Compositional model for the Earth's core. In: Holland, H.D., Turekian, K.K. (Eds.), Treat. Geochem. Pergamon, Oxford, pp. 547–568. https://doi.org/10.1016/B0-08-043751-6/02015-6.
Mei, Q.-F., Yang, J.-H., Yang, Y.-H., 2018. An improved extraction chromatographic purification of tungsten from a silicate matrix for high precision isotopic measurements using MC-ICPMS. Journ. Anal. At. Spectrom. 33, 569–577. https://doi.org/10.1039/C8JA00024G.
Moreira, M., Breddam, K., Curtice, J., Kurz, M.D., 2001. Solar neon in the Icelandic mantle: new evidence for an undegassed lower mantle. Earth Planet. Sci. Lett. 185, 15–23. https://doi.org/10.1016/S0012-821X(00)00351-4.
Mukhopadhyay, S., 2012. Early differentiation and volatile accretion recorded in deep-mantle neon and xenon. Nature 486, 101. https://doi.org/10.1038/nature11141.
Mundl, A., Touboul, M., Jackson, M.G., Day, J.M.D., Kurz, M.D., Lekic, V., Helz, R.T., Walker, R.J., 2017. Tungsten-182 heterogeneity in modern ocean island basalts. Science 356, 66. https://doi.org/10.1126/science.aal4179.
Mundl, A., Walker, R.J., Reimink, J.R., Rudnick, R.L., Gaschnig, R.M., 2018. Tungsten-182 in the upper continental crust: evidence from glacial diamictites. Chem. Geol. 494, 144–152. https://doi.org/10.1016/j.chemgeo.2018.07.036.
Murphy, D.T., Brandon, A.D., Debaille, V., Burgess, R., Ballentine, C., 2010. In search of a hidden long-term isolated sub-chondritic 142Nd/144Nd reservoir in the deep mantle: implications for the Nd isotope systematics of the Earth. Geochim. Cosmochim. Acta 74, 738–750. https://doi.org/10.1016/j.gca.2009.10.005.
Parman, S.W., Kurz, M.D., Hart, S.R., Grove, T.L., 2005. Helium solubility in olivine and implications for high 3He/4He in ocean island basalts. Nature 437, 1140–1143. https://doi.org/10.1038/nature04215.
Pedersen, A.K., Larsen, L.M., Pedersen, G.K., 2017. Lithostratigraphy, geology and geochemistry of the volcanic rocks of the Vaigat Formation on Disko and Nuussuaq. In: Geological Survey of Denmark and Greenland Bulletin. Paleocene of West Greenland, pp. 1–244.
Peters, B.J., Mundl-Petermeier, A., Horan, M.F., Carlson, R.W., Walker, R.J., 2019. Chemical separation of tungsten and other trace elements for TIMS isotope ratio measurements using organic acids. Geost. Geoan. Res. 43, 245–259. https://doi.org/10.1111/ggr.12259.
Puchtel, I.S., Blichert-Toft, J., Touboul, M., Horan, M.F., Walker, R.J., 2016. The coupled ^{182}W-^{142}Nd record of early terrestrial mantle differentiation. Geochem. Geophys. Geosys. 17, 2168–2193. https://doi.org/10.1002/2016GC006324.
Puchtel, I.S., Blichert-Toft, J., Touboul, M., Walker, R.J., 2018. ^{182}W and HSE constraints from 2.7 Ga komatiites on the heterogeneous nature of the Archean mantle. Geochim. Cosmochim. Acta 228, 1–26. https://doi.org/10.1016/j.gca.2018.02.030.
Rehkämper, M., Halliday, A.N., 1997. Development and application of new ionda-shexchange techniques for the separation of the platinum group and other siderophile elements from geological samples. Talanta 44, 663–672. https://doi.org/10.1016/S0039-9140(96)02100-5.
Reimink, J.R., Chacko, T., Carlson, R.W., Shirey, S.B., Liu, J., Stern, R.A., Bauer, A.M., Pearson, D.G., Heaman, L.M., 2018. Petrogenesis and tectonics of the Acasta Gneiss complex derived from integrated petrology and ^{142}Nd and ^{182}W extinct nuclide-geochemistry. Earth Planet. Sci. Lett. 494, 12–22. https://doi.org/10.1016/j.epsl.2018.04.047.
Righter, K., Shearer, C.K., 2003. Magmatic fractionation of Hf and W: constraints on the timing of core formation and differentiation in the Moon and Mars. Geochim. Cosmochim. Acta 67, 2497–2507. https://doi.org/10.1016/S0016-7037(02)01349-2.
Rizo, H., Walker, R.J., Carlson, R.W., Horan, M.F., Mukhopadhyay, S., Manthos, V., Francis, D., Jackson, M.G., 2016a. Preservation of Earth-forming events in the tungsten isotopic composition of modern flood basalts. Science 352, 809. https://doi.org/10.1126/science.aad8563.
Rizo, H., Walker, R.J., Carlson, R.W., Touboul, M., Horan, M.F., Puchtel, I.S., Boyet, M., Rosing, M.T., 2016b. Early Earth differentiation investigated through ^{142}Nd, ^{182}W, and highly siderophile element abundances in samples from Isua, Greenland. Geochim. Cosmochim. Acta 175, 319–336. https://doi.org/10.1016/j.gca.2015.12.007.
Saunders, A.D., Fitton, J.G., Kerr, A.C., Norry, M.J., Kent, R.W., 1997. The North Atlantic Igneous Province. In: Large Igneous Provinces: Continental, Oceanic, and Planetary Flood Volcanism. Geophysical Monograph Series.
Schilling, J.-G., Meyer, P.S., Kingsley, R.H., 1982. Evolution of the Iceland hotspot. Nature 296, 313–320. https://doi.org/10.1038/296313a0.
Skovgaard, A.C., Storey, M., Baker, J., Blusztajn, J., Hart, S.R., 2001. Osmium–oxygen isotopic evidence for a recycled and strongly depleted component in the Iceland mantle plume. Earth Planet. Sci. Lett. 194, 259–275. https://doi.org/10.1016/S0012-821X(01)00549-0.
Starkey, N.A., Stuart, F.M., Ellam, R.M., Fitton, J.G., Basu, S., Larsen, L.M., 2009. Helium isotopes in early Iceland plume picrites: constraints on the composition of high ^{3}He/^{4}He mantle. Earth Planet. Sci. Lett. 277, 91–100. https://doi.org/10.1016/j.epsl.2008.10.007.
Storey, M., Duncan, R., Pedersen, A., Larsen, L., Larsen, H., 1998. ^{40}Ar/^{39}Ar geochronology of the West Greenland Tertiary volcanic province. Earth Planet. Sci. Lett. 160, 569–586. https://doi.org/10.1016/S0012-821X(98)00112-5.
Thirlwall, M.F., Upton, B.G.J., Jenkins, C., 1994. Interaction between Continental Lithosphere and the Iceland Plume—Sr-Nd-Pb Isotope Geochemistry of Tertiary Basalts, NE Greenland. J. Pet. 35, 839–879. https://doi.org/10.1093/petrology/35.3.839.
Touboul, M., Puchtel, I.S., Walker, R.J., 2012. ^{182}W evidence for long-term preservation of early mantle differentiation products. Science 335, 1065. https://doi.org/10.1126/science.1216351.
Touboul, M., Liu, J., O'Neil, J., Puchtel, I.S., Walker, R.J., 2014. New insights into the Hadean mantle revealed by 182W and highly siderophile element abundances of supracrustal rocks from the Nuvvuagittuq Greenstone Belt, Quebec, Canada. Chem. Geol. 383, 63–75. https://doi.org/10.1016/j.chemgeo.2014.05.030.
Tusch, J., Sprung, P., van de Löcht, J., Hoffmann, J.E., Boyd, A.J., Rosing, M.T., Münker, C., 2019. Uniform 182W isotope compositions in Eoarchean rocks from the Isua region, SW Greenland: the role of early silicate differentiation and missing late veneer. Geochim. Cosmochim. Acta 257, 284–310. https://doi.org/10.1016/j.gca.2019.05.012.
Upton, B.G.J., Emeleus, C.H., Hald, N., 1980. Tertiary volcanism in northern E Greenland: Gauss Halvø and hold with Hope. Journ. Geol. Soc. 137, 491. https://doi.org/10.1144/gsjgs.137.4.0491.
Vockenhuber, C., Bichler, M., Golser, R., Kutschera, W., Priller, A., Steier, P., Winkler, S., 2004. ^{182}Hf, a new isotope for AMS. Nucl. Instrum. Methods Phys. Res., Sect. B 223–224, 823–828. https://doi.org/10.1016/j.nimb.2004.04.152.
Welke, H., Moorbath, S., Cumming, G.L., Sigurdsson, H., 1968. Lead isotope studies on igneous rocks from Iceland. Earth Planet. Sci. Lett. 4, 221–231. https://doi.org/10.1016/0012-821X(68)90039-3.
Wicks, J.K., Jackson, J.M., Sturhahn, W., 2010. Very low sound velocities in iron-rich (Mg,Fe)O: implications for the core-mantle boundary region. Geophys. Res. Lett. 37. https://doi.org/10.1029/2010GL043689.
Willbold, M., Elliott, T., Moorbath, S., 2011. The tungsten isotopic composition of the Earth's mantle before the terminal bombardment. Nature 477, 195. https://doi.org/10.1038/nature10399.
Willbold, M., Mojzsis, S.J., Chen, H.-W., Elliott, T., 2015. Tungsten isotope composition of the Acasta Gneiss complex. Earth Planet. Sci. Lett. Letters 419, 168–177. https://doi.org/10.1016/j.epsl.2015.02.040.
Williams, A.J., 2005. The Nature of the Chemically Enriched Components of the Iceland Mantle Plume. PhD Thesis. URI. http://hdl.handle.net/1842/14667.
Yuan, K., Romanowicz, B., 2017. Seismic evidence for partial melting at the root of major hot spot plumes. Science 357, 393. https://doi.org/10.1126/science.aan0760.